Recent progress in additive manufacturing of fiber reinforced polymer composite

Goh, Guo Dong; Yap, Yee Ling; Agarwala, Shweta; Yeong, Wai Yee

2018

Goh, G. D., Yap, Y. L., Agarwala, S., & Yeong, W. Y. (2019). Recent progress in additive manufacturing of fiber reinforced polymer composite. Advanced Materials Technologies, 4(1), 1800271-. doi:10.1002/admt.201800271

https://hdl.handle.net/10356/141841

https://doi.org/10.1002/admt.201800271

Recent progress in Additive Manufacturing of Fiber Reinforced Polymer Composite

G. D. Goh[1], Y. L. Yap[1], S. Agarwala[1], W. Y. Yeong[1*]

Singapore Centre for 3D Printing, School of Mechanical and Aerospace Engineering, Nanyang Technological University, 50 Nanyang Avenue, Singapore 639798

*Corresponding Author

Designation: Assistant Professor, Mechanical and Aerospace Engineering and Aerospace and Defence Program Director, Singapore Centre for 3D Printing, Nanyang Technological University, Singapore

Email: WYYeong@ntu.edu.sg

Tel: +65-67904343

Abstract

Additive Manufacturing (AM) has brought about a revolution in manufacturing complex products with customized features. It is finding application in everything from aerospace, automotive, consumer to biomedical as it evolves. AM of composites is especially attractive as it holds promise to improve, modify and diversify the properties of generic materials by introducing reinforcements. This article provides a detailed landscape of fiber-reinforced composites processed with AM techniques, discussing various AM processes, strengths, weaknesses and material formulations. AM techniques focusing on continuous fibers have been evaluated in-depth to cover all aspects; as these hold the promise of becoming the next-generation composite fabrication methodology. Potential future works and challenges in printing fiber reinforced polymer composites (FRPC) have also been identified.

Keywords: Additive manufacturing, 3D printing, Rapid prototyping, Fiber reinforced polymer composite

1. Introduction

Fiber reinforced polymer composites (FRPC) have been the cynosure of research and industry and they have found wide applications in automotive, aerospace, construction, sports and leisure owing to their high strength to weight ratio. Conventional manufacturing techniques employed to process FRPC are manual layup [1, 2], resin transfer molding (RTM) [2, 3], spray-up [4], automated tape laying (ATL) [5], automated fiber placement (AFP) [6], filament winding [7], and pultrusion [8]. However, one common issue with all conventional techniques is the need for molds, which is not only expensive to manufacture but also limit the formability of the part. As a result, producing complex and customized parts becomes tedious and costly.

The need for low-cost, automated fabrication process and design flexibility have spurred the development of additive manufacturing (AM) for FRPC [9]. AM refers to a group of fabrication techniques in which parts are fabricated layer by layer directly from CAD file [9]. AM, which does not require expensive molds, has simplified the way complex parts are designed and lowered the fabrication costs. The added flexibility of changing fiber volume fraction and the ability to have locally changing fiber orientations to create functionally graded structures would certainly make AM a lead technology in the composite industry. Development of short fiber reinforced polymers that exhibit superior strength for AM processes has been on-going for at least a decade. Recent researches have revealed the trends in developing new FRPC including continuous fibers, as well as AM process modification to allow the fabrication of parts with improved mechanical performance.

There are certain requirements that FRPC material needs to fulfill in order to be processed by AM, they are 1) Types of reinforcements and matrices; 2) good fiber-to-matrix bonding; 3) fiber homogeneity; 4) fiber alignment; 5) good interlayer bonding; 6) minimal porosity.

Fiber reinforcement of appropriate size, shape, and length needs to be selected to suit the intended purpose of the part. Both matrix material, which holds the fibers in place, and reinforcement, need to be compatible with the selected AM technique. A good fiber-to-matrix bonding is required at the fiber-matrix interface to allow loads to be transferred efficiently from the matrix, thus resulting in composites that follow the 'rule of mixture'. Fiber loading should also be optimized in order to obtain the best mechanical properties for AM composites. Homogeneity in fiber distribution is needed to ensure consistent properties throughout the printed part. Added ability to control fiber distribution and alignment in a predefined location and direction respectively also allows strengthening sections of an object. A good inter-layer fusion is required to avoid delamination. Lastly, unwanted voids that would affect the mechanical properties of FRPC should be minimized.

Several review papers on AM of composites [10-16, 17] have highlighted important aspects such as their use in bio-medical applications [13], opportunity and challenges of additive manufacturing of multi-directional preforms for composites [14], mechanical properties of AM short FRP composites and the use of composites in various industries [15], physics involved in fused filament fabrication [11]for composites, Four-Dimensional (4D) printing of active Polymer-Fiber composites [12], and development in nanocomposites [10] and composites materials for AM [17]. However, further review in other aspects such as AM of continuous FRP composites and current position of additively manufactured FRP composites in relative to conventionally manufactured ones in terms of mechanical properties also deserve merits. This paper serves to keep the readers abreast of the state-of-the-art AM of FRP composites. Research direction in AM techniques for fiber reinforced polymer FRP composite materials used are discussed based on the aforementioned 6 requirements to obtain successful additively manufactured FRP composites. In addition, the potential and challenges of AM of FRP composites are also highlighted.

2. Additive Manufacturing techniques for FRPC

AM techniques for FRPC are broadly classified into four processes, namely material extrusion, vat photopolymerization, sheet lamination and powder bed fusion, as per ASTM International Technical Committee F42 on AM technologies (fig. 1). Table 1 shows a summary of various AM techniques for FRPC.

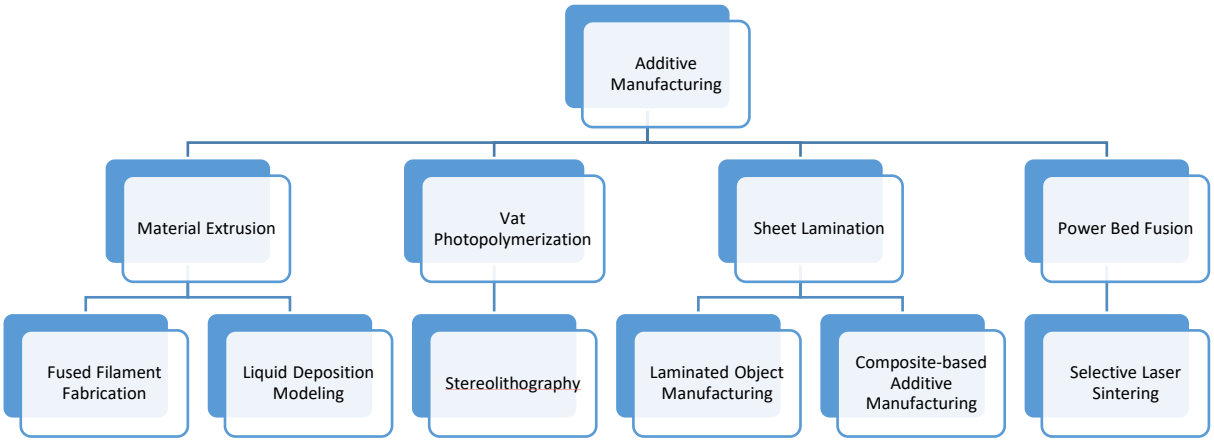

Figure 1 Classification of different AM processes for FRPC

Table 1 Summary of AM techniques showing types of base materials, advantages, disadvantages, special properties of the printed materials, fiber alignment and alignment methods

Techniques	Type of base materials	Advantages	Disadvantages	Special properties of printed materials	Fiber alignment	Alignment methods
Material extrusion (FFF, LDM)	FFF Continuous filaments of thermoplastic polymers LDM A concentrated dispersion of particles in a liquid (ink or paste) or epoxy resin	Low cost Easy fabrication Able to modify print-head for laying fibers Multi-material capability	Obvious layer-by-layer effect Nozzle degradation Nozzle clogging at high fiber volume	Electrically conductive [18, 19] Graded dielectricity [20] Electro-caloric deformation [21]	Along printing direction	Shear stress (during preparation of feedstock material)[22-25] Mechanical pulling and laying [26-28] Shear stress (against the nozzle wall) [29]
Vat photo-polymerization	A resin with photo-active monomers	Fine resolution	Very limited materials	Piezoelectric property [30]	Along electric-field direction	Electrical Polarization effect [32, 33]

(SLA)		Random alignment of discontinuous fibers for isotropic mechanical property	Adding fiber increases viscosity, thus making handling difficult Fiber sedimentation in resin Need for additional feeding device for deposition UV penetration issue Bubble formation causing pores to form and leading to crack initiation	Shape memory properties[31]	Along magnetic field direction Along laying direction According to fiber pattern of the mat Random orientation	Magnetic Polarization effect [34, 35] Acoustic effect[36] Shear induced[37] Mechanical Laying using Fiber dispensing device[38] Mechanical laying of mat [39, 40]
Powder bed fusion (SLS)	Compacted fine powders	Fine resolution Easy to remove support material Unused powder can be reused High loading of reinforcement	Slow printing Expensive High porosity in the binder method Long and continuous fiber reinforcement not possible Rough surface finish	Electrically conductive [41]	Random orientation[42]	-
Laminated object manufacturing **(LOM, CBAM)**	Polymer composite in sheet	High-strength parts can be produced Low cost No post processing	High material wastage Difficult to build complex internal cavities [43]	Excellent mechanical properties	Uniform fiber direction[44] Randomly aligned[45]	During the preparation of the feedstock composite sheet

	No need for support structures

2.1 Material Extrusion

Material extrusion process selectively deposits the composite material in the solid filament form or paste form, through a nozzle. The technique used to melt and extrude the filament is called fused filament fabrication (FFF) [46] whereas the one in which paste or fluid-like feedstock is printed is called liquid deposition modeling (LDM) [29].

2.1.1 Fused Filament Fabrication

This section focuses on various research carried out on developing new FRP composite materials, ranging from nano-scale discontinuous to continuous fibers using the FFF technique.

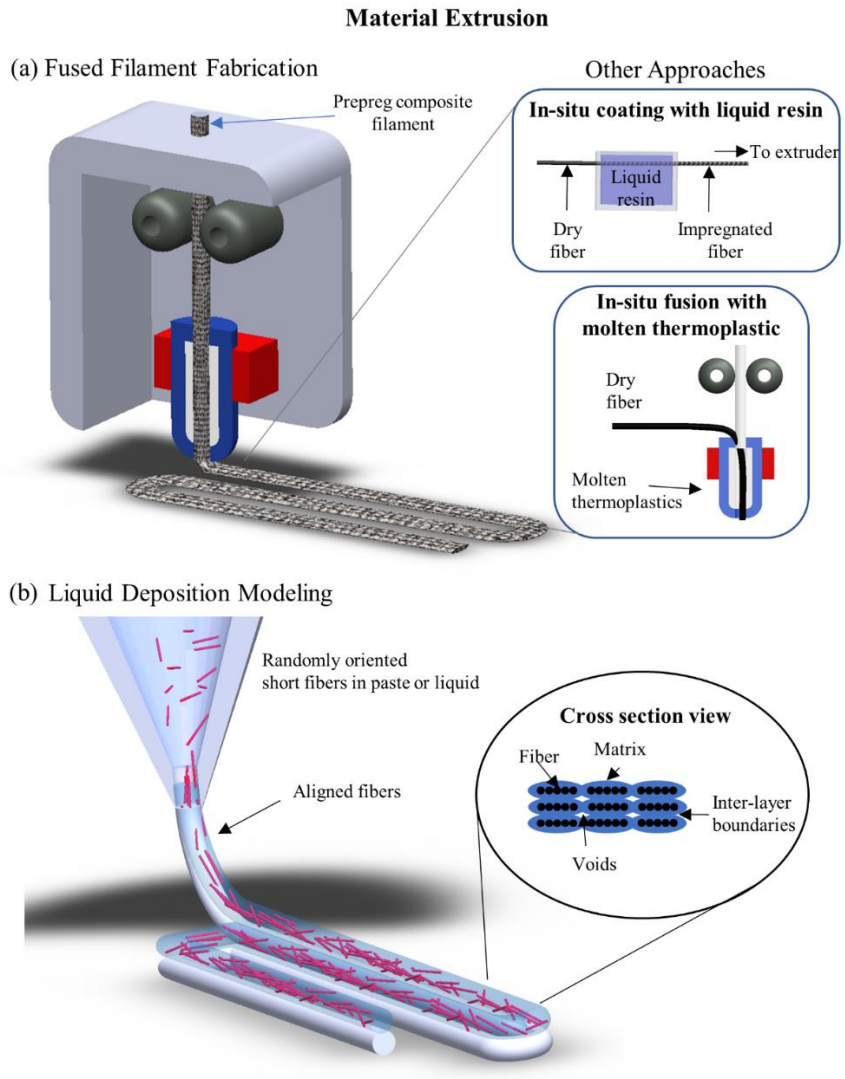

Figure 2 Material extrusion process: (a) three approaches to fabricate composite parts using fused filament fabrication, namely, extrusion of prepreg composite filament, in-situ coating of fibre with liquid resin, and in-situ fusion of fiber with molten thermoplastics. Nozzle is heated to melt the thermoplastic filament before being selectively deposited. (b) extrusion of randomly oriented short fibers in paste-like resin in liquid deposition modelling, alignment of fiber was due to shearing against the nozzle inner wall. Nozzle may or may not be heated up. Curing mechanism is needed in liquid deposition modelling.

2.1.1.1 Discontinuous fibers

Discontinuous fibers in varying sizes have been used for the FFF techniques. Among them are nano-scale single-walled carbon nanotube (SWNT) [24, 25], multi-walled carbon nanotube (MWNT) [47], vapor-grown carbon fiber (VGCF) [24, 25] and graphene [48, 49]; micron-sized metal powders, copper [10] and iron [10,11]; and millimeter long chopped fibers such as thermotropic liquid crystalline polymers (TLCPs) [50, 51], glass [52], and carbon [22, 23]. Natural fibers such as Harakeke and Hemp have also been used as reinforcement [53].The commonly

Acrylonitrile Butadiene Styrene (ABS) (230°C) [22-25, 48, 49, 52, 54, 55], nylon (245-265°C) [56], polylactic acid (PLA) (180°C to 220°C) [47, 49] and polypropylene (PP) (170-220°C) [50, 51], and material that require high processing temperature such as Ultem® (375-420°C) [57] and Polyether ether ketone (PEEK) (350°C to 420°C) [58] .

Initially the fibers are not fully aligned in the composite filament, but shearing force between fibers and nozzle walls give rise to alignment during the AM process [24, 25]. Long fibers generally provide improved mechanical properties [54]. Adding 13 wt% millimeter-sized carbon fiber reinforcement [22] has noted greater improvement in the in-plane tensile strength and modulus by 250% and 400%, respectively, than that with 10 wt% nano-scale SWNT reinforcement (39% and 61% respectively) [24]. The improvement is attributed to the larger surface area that permits higher shear at the fiber-matrix interface, thus allowing longer fibers to bear significantly higher load. However, the mechanical properties of the discontinuous FRPC (table 2) remain inferior to composites fabricated by conventional sprayup process, which can go as high as 270 MPa [59] which is illustrated in Fig. 3.

Effect of fiber loading is another area that has been studied and it is found to be dependent on the reinforcement-matrix combination. Mechanical properties such as elastic modulus tend to increase with fiber loading at low loading ratio, but deteriorate after reaching an optimum value [23]. This phenomenon generally occurs due to poor wettability of fiber with thermoplastic which leads to poor fiber-matrix interface. Moreover, higher loading causes viscosity to increase and decreases the flowability [60, 61], thus causing processability issues such as nozzle clogging (~40 wt%) [23, 48, 49]. Surfactants and plasticizers can be added to improve fiber-to-matrix bonding and the process ability of the material. For instance, linear low-density polyethylene (LLDPE) and hydrogenated Buna-N were added as toughening and

LLDPE and 1 wt% of hydrogenated Buna-N, the tensile strength can be improved by 50%.

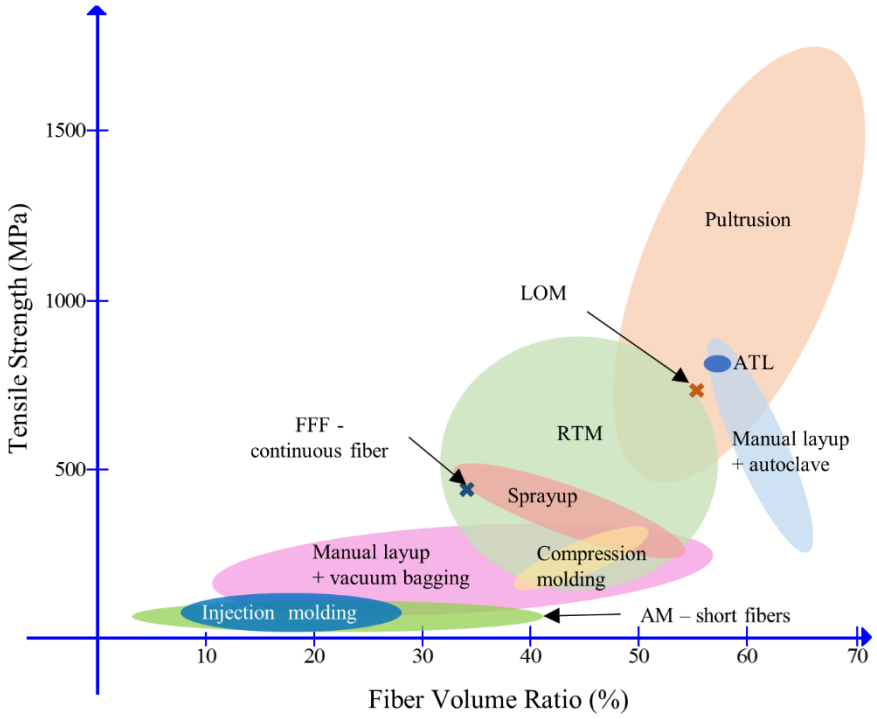

Figure 3 Tensile strength vs fiber volume ratio of parts manufactured via various conventional and AM techniques

The addition of fibers weakens the inter-layer fusion, contrary to what was expected. The out-of-plane tensile strength of the composites (7 MPa) was found to be lower than that of the unreinforced thermoplastics (16.75 MPa) [22]. This could be due to the low conformity of the fibers to the previous layer, thus reducing the contact area between layers. In addition to that, the fibers are aligned within a layer and not across the layer making them not able to reinforce the out-of-plane tensile strength.

Berratta et al. tested the tensile stress of CNT/PEEK composite filament and the printed parts [62]. It was found out that although the tensile strength of the composite filament shows improvement with the increasing CNT content, the tensile strength of the printed parts decreases at higher CNT content (5wt%). It was found out that the more pores were observed

in the printed parts with 5wt% CNT content as compared to the printed part with 1wt% CNT content. This shows that there is an interaction between the reinforcement and the matrix during the extrusion process which would introduce air gap which can be detrimental to the mechanical properties. This warrants further investigation to further reduce the void formation.

Short FRPC are relatively easier to be processed by FFF as they are extruded in normal filament from without the need for extra fiber laying mechanism. FFF, however, suffers from limitations like porosity and voids. Voids have been observed to form in between the extruded filaments, thus leading to delamination and reducing the tensile strength [23]. Reinforcement is also more effective along the direction of the filament as compared to across the layer direction as fibers tend to align along the extrusion direction resulting in high anisotropy in mechanical properties [48].

2.1.1.2 Continuous fibers

Much work has been done to fabricate continuous FRPC using PLA [63, 64], ABS [27, 28, 65-67], nylon [26, 68] and Ultem® as the matrix, and carbon [26, 64], glass [67], and Kevlar fibers [68] as the reinforcement. AM processing of continuous fiber can be done by simply modifying the print head. Different approaches to print continuous fiber FRPC have been demonstrated (fig. 2(a)), such as i) in-situ fusion of thermoplastic liquid resin before extrusion [67]; ii) in-situ fusion of molten thermoplastic with fibers at the nozzle [27, 28, 63-66] and iii) extrusion of pre-impregnated fibers [26, 68, 69]. In (i), glass fibers pass through the solution containing dissolved ABS [67]. It is discovered that viscosity would affect both the resin content and the traction force to pull the fibers impregnated within resin. In (ii), fibers are fused into molten thermoplastic filament at the nozzle [27, 28, 63-66]. The fibers are extruded automatically, without any feeding device as they tend to be drawn into the nozzle by the movement of melted thermoplastic. In (iii), continuous fiber bundle pre-impregnated with thermoplastics such as nylon and Ultem®

are directly fed and extruded from the nozzle. Mechanisms like mechanical cutting [26], laser cutting and resistive heating [69], are needed to cut the fibers at the end of each layer. Comparing to unreinforced specimens, reinforcement by continuous fibers brings about significant improvement (by as much as 5 times) in the tensile properties [26, 70-72].

However, like discontinuous fiber, higher loading of continuous fibers also leads to nozzle clogging. Nozzle clogging issue could be potentially solved by having a separated laying mechanism for fiber, such that the fiber is directly encapsulated by the extruded thermoplastic [18]. Moreover, high fiber loading weakens the inter-layer fusion, resulting in low inter-laminar shear strength [27]. In addition to inter-layer fusion, fiber-matrix interface also needs to be improved for printing continuous FRPC. It was found out that higher temperature during extrusion and post-process like thermal bonding can help to reduce the viscosity and improve impregnation [65, 66].

2.1.2 Liquid Deposition Modeling

For composite feedstock in the form of paste or fluid, the materials are selectively deposited from a syringe that is attached to the computerized numerical control (CNC) machine (fig.2 (b)). To date, reinforcements only exist in the form of discontinuous fibers in the composite feedstock.

2.1.2.1 Discontinuous fibers

Thermoplastics such as PLA [73] and thermosets such as acrylic-based and epoxy-based resins have been used as the matrix material [74, 75]. So far, the reinforcement exists only in form of discontinuous fibers like silicon carbide (SiC) whiskers [29] , carbon fibers [29, 74, 75] , glass fibers [74] and carbon nanotubes (CNT) [73, 76]. Reinforcement materials are mixed homogeneously with liquid resin to form paste-like composite feedstock. Some reinforcements especially CNTs

generally suffer from problem of agglomeration, it is hence essential to do surface treatment with acid to ionize the CNTs or to use suitable solvent mediums such as polyvinylpyrrolidone to uniformly disperse them [76].

Being in liquid form at room temperature, it is generally easier to process thermoset resins than the thermoplastics using LDM technique. Epoxy resin ink, however, requires specific rheological and viscoelastic properties to be extruded smoothly from the nozzle. It should be noted that most ink dispersions formed using these materials exhibit a shear-thinning behavior characterized by increasing shear rate with decreasing viscosity [76].

In another variation, photo-curable and thermo-curable components are added to form dual-cure composites, where the former allows fast curing to maintain the shape while the latter helps to complete the crosslinking to achieve good mechanical properties [74, 75]. Imidazole-based ionic liquids has been explored to use as a curing agent to prolong the printing window to up to 30 days under ambient conditions [29]. It has been shown that use of volatile solvents for dissolving thermoplastics lowers the processing temperature [29].

The work on epoxy-based resins is of significance as it demonstrates how fibers can be aligned by controlling parameters like aspect ratio and nozzle diameter [29]. Although only discontinuous FRPC have been printed so far, the efforts mark an important step in designing engineering materials and can be manipulated to print continuous fibers in the future.

2.2 Vat Photopolymerization

Vat photopolymerization selectively cures photopolymer in a vat using ultraviolet (UV) light. Stereolithography (SLA) is a commonly used vat photopolymerization technique to print FRPC (fig.4).

2.2.1 Stereolithography

To date, reinforcements in the forms of discontinuous fibers, continuous fibers and fiber mat have been used in SLA to create FRPC. SLA is known to produce parts with low porosity (0-5%) [34, 77, 78].

2.2.1.1 Discontinuous fibers

Various types of discontinuous reinforcements ranging from nano-scale fibers, for example, silicate dioxide (SiO_2) nanoparticles [79], graphene oxide [80] and carbon black [81], micron-scale fibers, for example, alpha-alumina powder [82], ferromagnetic fibers [34, 35], titanium carbide (TiC) [32], bioglass [78] and SiC [83], and to milli-scale glass fiber [77, 84, 85] have been used to create FRPC in SLA. Matrix materials used are generally photosensitive polyacrylate resin [77-79, 85, 86], although polyester resin [87] and epoxy resin [88] have also been attempted.

There are mainly two methods to prepare the composite materials, i.e. i) by premixing the reinforcement and resin [32, 34, 77-79, 81, 83, 86, 88, 89] and ii) dispersing the fiber on the surface of resin [85]. Additives may be added into the composite for various reasons, namely to facilitate polymerization, reduce viscosity of the resin, stabilize the suspension, and to act as a coupling agent between the fiber and matrix. In another variation, a new layer of composite resin is added onto the build tray at the start of each layer to avoid sedimentation of fiber in the resin (Fig. 3b) [90-93]. The fiber surfaces are treated in order to decrease the viscosity of resin to permit higher fiber concentration. The highest tensile strength reported so far is 72 MPa with the addition of 16 vol% of glass fiber [92], implying that SLA fabricated FRPC is, nevertheless, still inferior to the conventional FRPC.

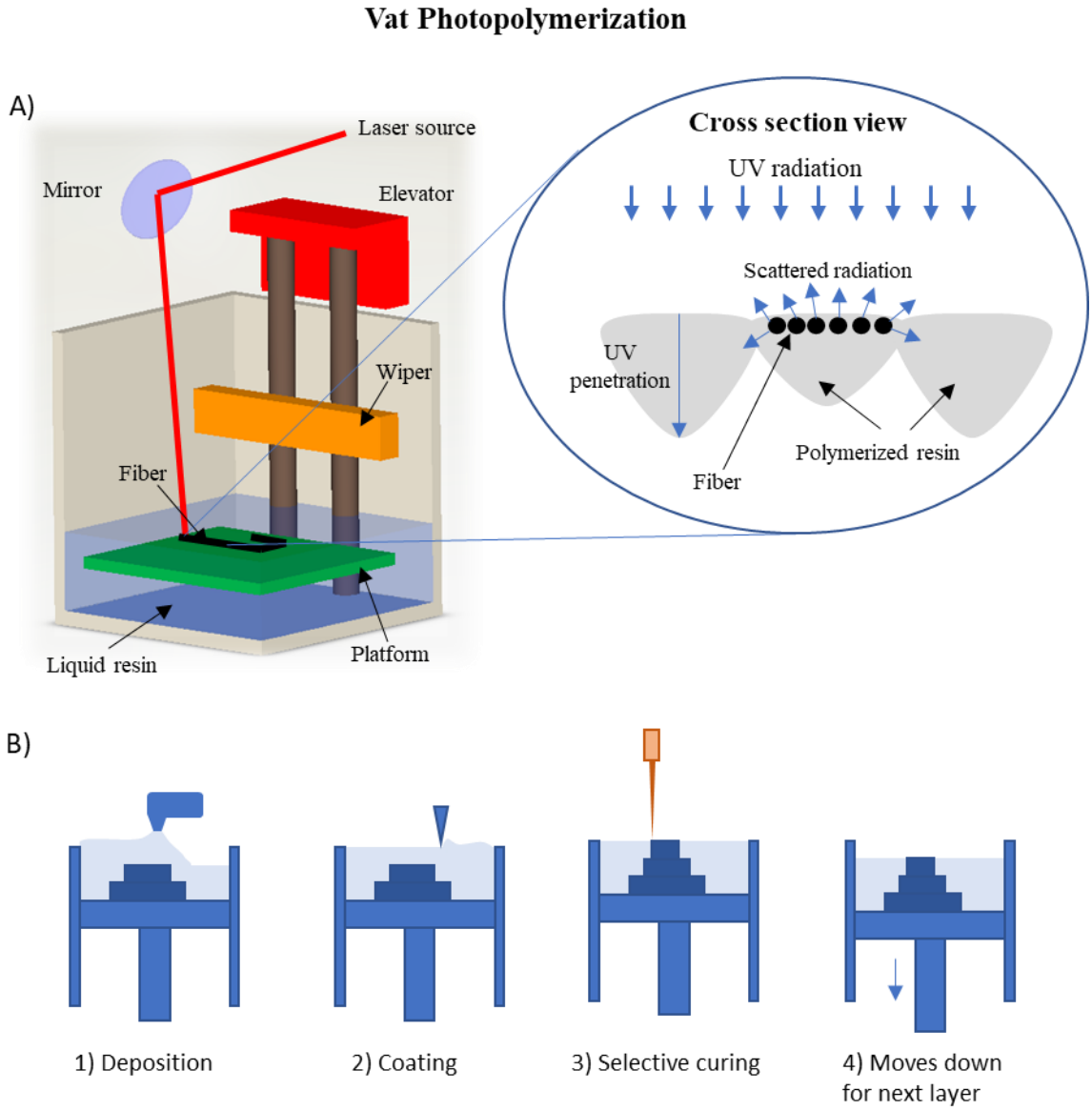

Figure 4 A)Vat-photopolymerization process and the schematic representation of the cross-sectional view of the UV curing of FRPC in SLA. Laser source in the UV spectrum is used. For continuous fiber, the fiber is laid either manually or automated. For short fiber, the fibers are premixed with the liquid resin. Addition of fibers reduces the UV penetration which requires modification of printing parameters. B) procedure of modified SLA in which new layer is deposited on top to prevent sedimentation of fibers

As the composite materials are normally premixed, fibers are randomly oriented and uniformly dispersed, resulting in the need for extra mechanism to align the fibers [77, 79]. Although fiber loading up to 60 vol% have been attempted, it was found that higher loading would generally lead to a poorer fiber dispersion [83]. In addition, entanglement of fibers is noticed at higher loading, which weakens the fiber-matrix bonding.

Improvement in tensile strength [77, 81], Young's Modulus [79], flexural strength [83], fracture toughness [79, 83], and hardness [88] have been observed upon adding reinforcement. However, these mechanical properties are influenced by the shape, density and size of the reinforcement. Unlike aforementioned cases, addition of microsphere was found to have negative effect on the tensile strength [85, 86]. The drop in tensile strength were probably due to the use of low density hollow microsphere. Lu et al. varied the carbon fiber length and found out that the fracture toughness was enhanced using 2 mm fibers while the flexural strength was higher with 1 mm fibers [83]. Apart from that, adding reinforcement minimizes the shrinkage and thus improving the printing quality [79].

However, there are several issues associated with the addition of reinforcement into the photo-curable resin. Firstly, the viscosity of the resin increases with the addition of the reinforcement, which may affect processability [79]. The light scattering caused by the particles in the suspension reduces the UV penetration depth and lateral resolution so longer irradiation [82] or higher laser power [77] is required to achieve the same polymerized depth. The issue can be circumvented by using materials that are transparent to the UV radiation, such as the aluminum-based quasicrystalline [88]. Post-curing is normally needed to complete the curing process as resin is not fully cured right after the printing. Chiappone et al. found out that post UV and thermal treatments would aid the reduction of graphene oxide which further enhances the stiffness of the SLA-fabricated graphene-based composite by as much as 126%[80].

2.2.1.2 Continuous fibers

Research has been carried out on continuous FRPC using glass [85] and carbon fiber bundles [38, 94] and e-glass and carbon fiber mats [39, 40] as reinforcement. Continuous fiber AM in SLA has been done by manual laying [39, 40, 85] or incorporating fiber laying mechanisms [38, 94].

The addition of continuous fiber has shown improvement in the tensile strength of the pure resin by 2-3 times [94]. In another work, E-glass, carbon and aramid nonwoven mats are used to reinforce acrylic- and epoxy-based resins [40]. It is found that E-glass and carbon in acrylic-based resin could bring about 50% improvement in both elastic modulus and tensile strength. However, the reinforcement loading achievable is low (<20%) due to the lack of consolidation process [85]. Although tensile strength between 83.5-143 MPa is obtainable, it still is short of the predicted strength due to poor fiber-matrix bonding [94]. The poor bonding is a result of incomplete curing in the interior due to the scattering of UV radiation caused by the fiber tows. In order to improve the fiber-matrix interface, thermal treatment [38] and post UV curing [39] are used to post-cure the resin. It was found that the tensile strength improved from 46.0 MPa to 61.3 MPa as a result of thermal treatment indicating existence of uncured liquid resin in the interior of the fiber reinforced samples resulting from only photocuring of carbon fiber. Hence, the use of fibers that is transparent to UV radiation could be a potential solution to the problem. However, one of the problems of post curing is the internal stresses that are developed which lead to shrinkage and warpage of parts [95]. Apart from that, Placement of the continuous fiber or fiber mat is a problem, which may cause air entrapment [39] and cause uneven surface in printed part [94], thus weakening the inter-layer bonding.

2.3 Sheet Lamination

In sheet lamination, sheets of material are bonded to form an object. There are two techniques under this, namely laminated object manufacturing (LOM) and composite-based additive manufacturing method (CBAM).

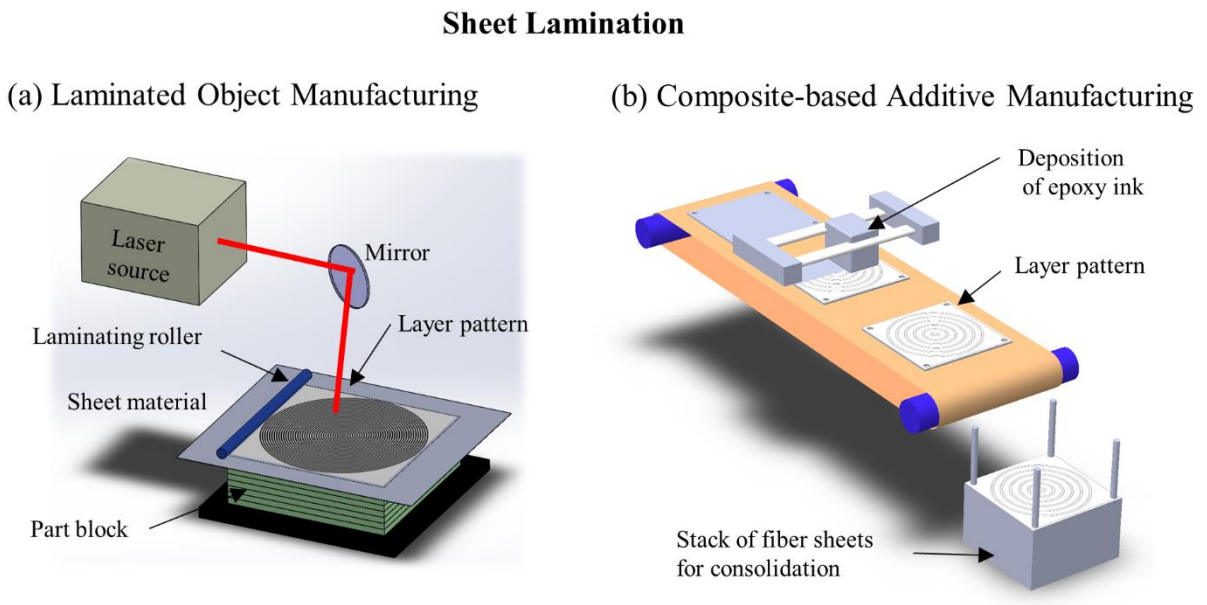

Figure 5 Sheet lamination process: (a) laminated object manufacturing (LOM) and (b) composite-based additive manufacturing. In LOM, laser source is used to cut out the layer pattern. Adhesive is applied to the whole area of the layer to bond the sheet. Pressure and heat are used to reduce the void content. Unwanted material will then be removed. In composite-based additive manufacturing, adhesive is selectively deposited according the pattern of each layer. The sheets are then stacked together and consolidated in oven. Unwanted material will then be removed.

2.3.1 Laminated Object Manufacturing (LOM)

LOM is a process that combines additive and subtractive techniques to build a part layer-by-layer from a stack of fiber sheets [43]. A laser is used to cut the shape of each layer and the layers are then bonded together by adhesive or by pressure and heat to reduce the void content (fig. 5(a)).

2.3.1.1 Mat/sheets

The feedstock to the LOM is in the form of sheet material, which can be commercial prepreg sheets or any fiber preform. Using prepreg sheets containing 55 vol% unidirectional E-glass fibers with epoxy matrix, tensile strength and flexural strength of the LOM fabricated FRPC are found out to be 716 MPa and 1.19 GPa respectively indicating good fiber-matrix and inter-layer bonding [44]. The LOM process is further improved by integrating a curved layer building mechanism, which eradicated stair-step effect, minimized wastage, and provided the capability to keep continuous fibers in the direction of curvature [96].

2.3.2 Composite-based additive manufacturing method (CBAM)

2.3.2.1 Mat/Sheet

CBAM utilizes an aqueous-based solution to be deposited first on each layer of fiber sheet using inkjet technique (fig. 5(b)). Subsequently, the fiber sheet is covered with thermoplastic powder matrix, which adheres only to the aqueous solution. After removing the excess powder, the fiber sheets are stacked, compressed, and heated in the oven to fuse the matrix for consolidation. Finally, the part is sandblasted to remove the excess fibers, revealing the final product. The highest tensile strength achievable so far is 165 MPa [45]. Low strength of CBAM printed part, when compared to LOM, is due to the use of randomly oriented discontinuous fiber sheets [97].

The ability to produce high strength parts compared to conventional methods is one of the advantages of sheet lamination technique. In addition, this technique does not require any support structure as the sheets can act as the support. However, unlike other AM processes where support structure is generated for overhanging features, the fiber sheets are needed in every layer. This leads to material wastage, as the used sheets are not reusable. Moreover, this technique does not allow complex internal features to be fabricated as the removal of unwanted materials would be difficult [43].

2.4 Powder bed fusion

Powder bed fusion makes use of thermal energy to selectively fuse regions of a powder bed. A commonly known powder bed fusion process for polymers is selective laser sintering (SLS) (fig.6).

2.4.1 Selective Laser Sintering

To date, reinforcements for SLS-fabricated FRPC are mostly found in the form of discontinuous fibers.

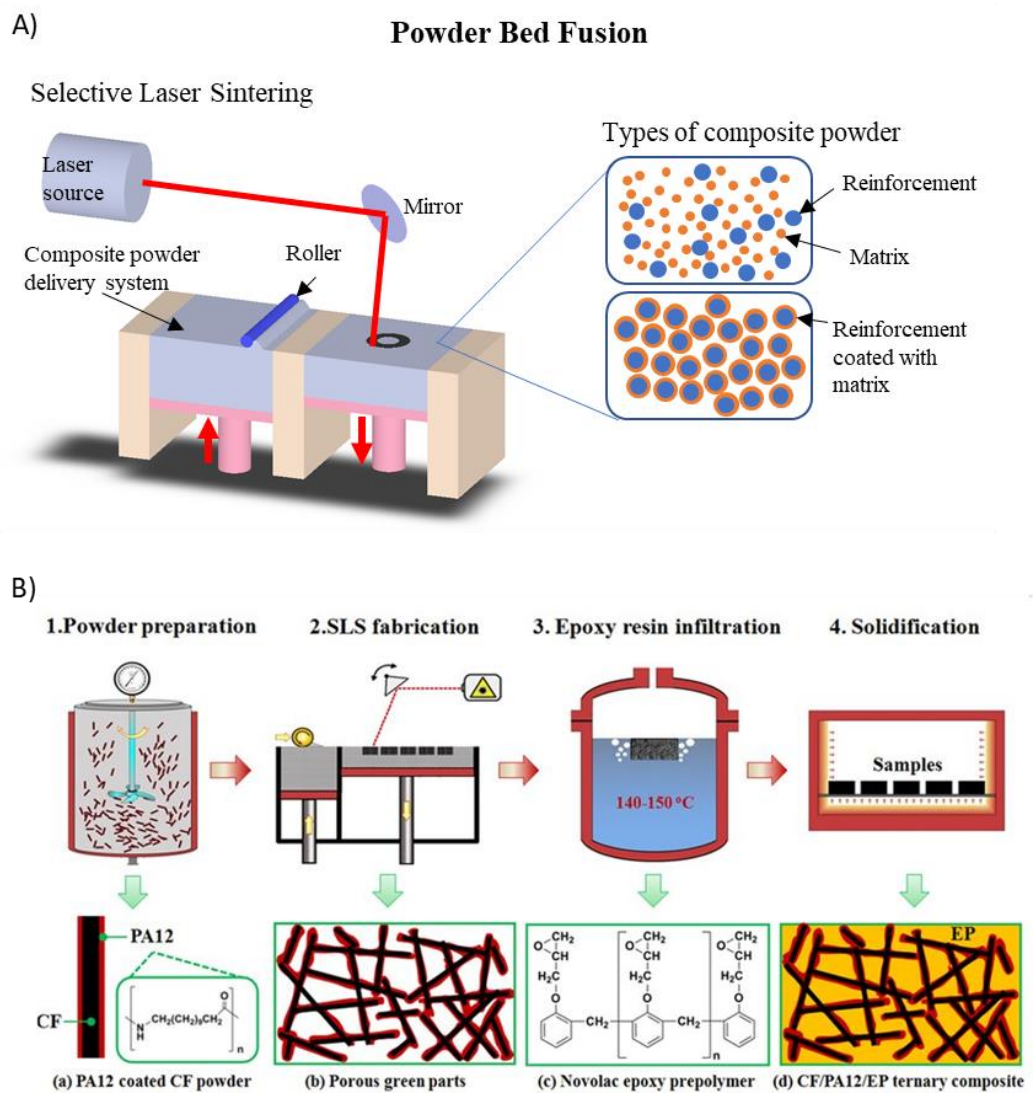

Figure 6 a) Schematic representation of powder bed fusion and the composite powder used. Composite powder can exist in two forms 1) homogeneously mixed reinforcement and matrix powders and 2) reinforcement powder precoated with matrix. A roller is used to lay a layer of powder onto the print platform. Laser is used as a heat source to selectively melt the composite powder. b) steps to fabricate carbon fiber reinforced epoxy composite using SLS 1) powder preparation 2) SLS fabrication 3) epoxy resin infiltration 4) solidification (retrieved from Zhu et al.)[98]

2.4.1.1 Discontinuous fibers

Many attempts to improve mechanical and physical properties by reinforcing raw powder with nano-scale and micro-scale fibers such as CNT [41, 99], carbon black [100], carbon nanofiber [42], yttrium stabilized zirconia (YSZ) [101], glass beads [102, 103], SiC [104, 105], and nanosilica [106] have been carried out. Various composite PA-12 powder are available commercially, namely glass-filled PA-12 (Duraform GF, PA3200 GF), carbon-fiber-filled PA-12 (Duraform HST, CarbonMide, Windform XT) and aluminum-filled PA-12 (Alumide).

Matrix materials used are typically the thermoplastics like polyamide, with PA-12 being most widely used in SLS [42, 101], although some other material such as polystyrene is also noted [107]. Instead of modifying the manufacturing process, research is targeted at homogeneously mixing the composite powder. This is achieved by using either mechanical [102, 105] and melt mixing [42] of the materials or by coating the fibers by dissolution-precipitation [106, 108] and surfactant-facilitated latex methods [41]. Recently, Zhu, Yan, Shi, Wen, Liu, Wei and Shi [98] developed short carbon fiber (CF) reinforced thermosetting composite by infiltrating the porous SLS manufactured PA-12/CF with epoxy resin under high temperature and pressure. Unlike other methods, the composite powder is prepared by coating a thin layer of PA-12 on the CF surfaces to produce a porous green-part before infiltration of epoxy resin (Fig. 5b).

Although adding reinforcement leads to enhancement in tensile modulus [109]; weak interface as a result of poor adhesion and voids is also observed [42, 110]. Though SLS fabricated pure PA-12 parts are generally stronger than those made by extrusion and injection molding, the SLS fabricated FRPC has significantly lower elastic modulus (1000MPa) and strength (28 MPa) than the ones made by conventional methods (1400 MPa and 42 MPa respectively)[100]. This was found to be due to poor dispersion of fibers in the powder feedstock and higher internal porosity predominantly present in the fiber-rich domains. The effect of laser intensity on the mechanical properties was investigated by Arai et al. [110]. It was found that increasing the laser intensity was necessary to lower the viscosity to improve the surface adhesion with the glass fiber. The optimum laser intensity was found to be around 22.7 kJ/m^2. However, further increase in laser intensity would degrade the mechanical properties due to the decrease in molecular weight of composite-copolymer poly(butylene terephthalate) powder. SLS is also restricted to developing discontinuous FRPC due to its fabrication nature [97]. If SLS is to be explored for laying continuous fibers, additional devices would be required to lay fibers and this would complicate the entire manufacturing process.

Table 1 Mechanical properties reported in literature

Techniques	Types of fiber		Fiber/ matrix composition	Mechanical Properties			Ref
				UTS (MPa)	Young's Modulus (GPa)	Other Properties and improvements due to addition of fibers	
FFF	Discontinuous	Nano	SWCNTs (5%)/ Carbon fiber (5%)/ MAGNUM 213 ABS	30	1.75	High reinforcement and better strength.	[24, 25]
			Graphene (5.6 wt%) /ABS/PLA	-	-	High mechanical strength	[49]
			MWCNTs (0.2%)/ PLA	55	3	47% increase in tensile strength	[47]
			Graphene nanoplatelets (4 wt%)/ ABS	35.5	2.8	Higher tensile modulus	[48]
			CNT (6wt%)/ABS	47.1	2.625	Conducted creep and electrical studies	[61]
			CNT (0.5wt%)/PLA	80	1.99		[111]
			CNT(1wt%)/PEEK	70		Short beam shear strength:21 MPa	[62]
		Micro	Fe_3O_4 (30–80 μm) (30-40%)/ P301 Nylon	4	0.054	Improved stiffness and thermal properties	[56]
			Cu (10 or 45μm)/ Fe (45 μm)/ ABS	15	0.23	Tensile modulus: 54 MPa with 30% Fe	[55]
			Short fiber (15%)/ ABS	42	2.5	Toughness: 6.3 $Jm^{-3}10^3$	[54]
			Harakeke (12.3 μm) (10-30%)/ /PP	25	0.32		[53]
			Hemp (28.3 μm)(10-30%)/ PP	15	0.3		
			Glass fiber (4%)/PLA	30	4	Impact strength: 60 J/m	[112]
		Milli	Vectra A950 TLCP (60 mm) (28%)/ Amoco polypropylene	45	4	High tensile modulus	[50, 51]
			Glass fiber (18%)/ ABS	58.6	-	Improved ductility and flexibility	[52]
			Carbon fiber (0.2-0.4 mm) (40%)/ ABS	65	14	115% higher tensile strength	[23]
			Carbon fiber (3.2 mm)/ ABS	70	8.91	Increased strength and stiffness	[22]
			Carbon fiber (15–20 mm) (10 wt%)/PA 12	90	3.5		[60]
			Carbon fiber / ABS	38	5.9	Shear strength: 13 MPa	[113]
	Continuous		Carbon fiber (34.5%)/nylon	475	35.7	High tensile modulus	[26]
			Carbon fiber bundle/ ABS	-	-	Increased strength	[65]
			Carbon fiber bundle/PLA	90	5.8	Tensile modulus: 294 GPa	[64]
			CNT yarn/ Ultem® 1010	117	2.4	Tensile strength: 317 MPa	[69]
			1000-carbon fiber bundle/ ABS	150	4	Flexural strength: 125 MPa Flexural modulus: 7.8 GPa Interlaminar shear strength: 2.81 MPa	[27, 28]
			Kevlar (10%) / Nylon	90	9	Elastic modulus: 1767 MPa	[68]
			Carbon fiber / PLA	91	-	Flexural strength: 156 MPa	[63]
			Carbon fiber(3000 fibers in a bundle)/epoxy resin	792	161		[72]

			Carbon fiber (48.93 vol%)/Nylon			Compressive strength: 53.3MPa Flexural strength: 231.1 MPa Flexural Modulus: 14.17	[114]
			Recycled Carbon fiber (8.9 vol%)/ PLA	260	20	Flexural strength: 263 MPa Flexural Modulus: 13.3 GPa Impact strength: 40 kJ/m^2)	[115]
			Carbon fiber (41 vol%)/ Nylon	600	13	Flexural strength: 430 MPa Flexural Modulus: 38.1 MPa Quasistatic indentation energy: 6.26 kJ	[71]
			Kevlar Fiber (35 vol%)/Nylon	450	7.2	Flexural strength: 149 MPa Flexural Modulus: 14.7 MPa Quasistatic indentation energy: 7.05 kJ	
			Carbon fiber/ Nylon	701	68.08	Poison ratio: 0.35 Compression strength at 0°: 223.06 MPa Compression strength 90°: 41.83 MPa	[70]
			Glass fiber/ Nylon	574.58	25.86	Poison ratio: 0.37 Compression strength at 0°: 82 MPa Compression strength 90°: 12.73 MPa Shear strength: 67.77 MPa	
			Carbon fiber (200 μm) (16.8wt%)/ABS	50	7		[116]
			Carbon fiber (200 μm)) (12.6wt%)/PLA	69	9		
			Carbon fiber (200 μm)) (17.7wt%)/PETG	69	8.5		
			Carbon fiber/ Nylon			Impact strength: 82.26 kJ.m^2	[117]
			Kevlar fiber/ Nylon			Impact strength: 184.76 kJ.m^2	
			Glass fiber/ Nylon			Impact strength: 280.95 kJ.m^2	
			e-glass fiber (54.8 wt%) / PP			Flexural modulus: 13.06 GPa	[118]
Liquid deposition modeling	Discontinuous	Micro	SiC whiskers/epoxy using an Epon 826 epoxy resin, nano-clay platelets, and dimethyl methyl phosphonate (DMMP)	Longitudinal: 96.6 Transverse: 69.8	Transverse: 10.61 Lonitudinal: 16.10	Young's modulus nearly equivalent to wood cell walls	[29]

			SiC whiskers-carbon fibers/ epoxy (Epon 826), nano-clay platelets, and dimethyl methyl phosphonate (DMMP)	Longitudinal: 66.2 Transverse: 43.9	Transverse: 8.06 Longitudinal: 24.5		
			Carbon Fibers (length 100-150 mm)/ Bisphenol A ethoxylate diacrylate/Bisphenol A diglycidyl ether/2,4,6- trimethylbenzoylphenyl phosphinate (Irgacure TPO-L)	40	3.6	Using dual-cure technique	[74, 75]
		Nano	A-MWNT (7 wt%)/ PVP (17 wt%)	-	-	Electrical Conducting	[76]
			MWCNTs (1 wt%) and PLA (30 wt%)	-	-	Electrical Conducting	[73]
SLA	Discontinuous	Nano	SiO_2 nanoparticles (20 nm)/ acrylate functionalized oligomers Genomer 4302 (G4302)/ Sartomer CN922 with the monomer tris(2-hydroxyethyl)isocyanurate triacrylate (SR368)	-	1.7	Fracture Toughness K_{1C} : 0.38 MPa $m^{-1/2}$	[79]
			Nano-carbon black (30 nm)/ Visible light curing polymer	0.24	-	Hardness: 81 mm Decomposition temperature: increased to 359.23°C	[81]
			Graphene Oxide (thickness 0.7–1.2 nm) (0.3 phr) / PEO-diacrylate		0.0116	Compression modulus: 9.6 MPa	[80]
			Graphene Oxide (thickness 0.7–1.2 nm) (0.5 phr) / PEO-diacrylate		0.0110	Compression modulus: 11.1 MPa	
		Micro	Hollow microsphere (55 μm)/ polyacrylate resin	-	-	Reduced tensile stress by using low density microsphere	[85]
			Alpha-alumina powder (P172SB, Pechiney)/ photocurable monomer	-	-	Improved vertical resolution	[82]
			Ferromagnetic fibers (γ Fe_2O_3)/ photopolymer	-	-	Magnetic alignment	[34, 35]
			Electrical conductive whisker (TiC) (50 μm)/photopolymer	-	-	Electric alignment	[32]
			Bioglass (5-30 μm)/ Acrylate-based monomer	-	-	Biaxial strength: 40 MPa	[78]
			Al59Cu25.5Fe12.5B3 (25 μm)/ Accura Si40 resin	-	-	Improvement in shrinkage improves by 90%	[88]
			Irregular SiC powders(40-53%)/ DSM Somos 19120 resin	-	-	Flexural Strength: 325 MPa Fracture toughness: 4.5 MPa $m^{1/2}$	[83]

		Milli	e-glass fiber (10-15 mm)/ polyacrylate resin	26	-	Provide better mechanical improvement compared to microsphere	[85]
			e-glass epoxy (80%)/ SLA 250 photopolymer	24.13	5.8	Functional graded materials with thermal and electrical conductivities can be created	[84]
			Glass fiber (20%)/ DeSolite SCR310 (SCR-310, 1995), a urethane acrylic based photo-polymer	29	3	Improved shrinkage	[77]
			Glass fiber (17.9%)/Ciba-Geigy SL5170 resin	72	2.49	60 percent increase in the modulus for the (riveted) composite specimens	[90, 91, 93]
			800 e-glass fibers (4.6%)/ Somos 3100 resin	87.2	3	twofold improvement of resin strength and stiffness	[119]
	Continuous		Thornel T-300 tow of 3000 fibers (5%)/ XB5081 Ciba Geigy	46.3	-	30% improvement in tensile strength	[38]
			Nonwoven fiber mat (e-Glass, PAN-based carbon, Aramid)/ Acrylic based matrix (AlliedSignal Exactomer 2202SF) or Epoxy based matrix (DSM Somos 7110)	30-55	1.81-2.85	increase of 36% in ultimate tensile strength	[39, 40]
LOM	Mat/ Sheet		Aerospace-grade prepreg containing e-glass fibers (52–55 vol%) / epoxy	713	-	Compression 896 MPa Flexure: 1190 MPa Interlaminar shear strength: 42.6 MPa	[44]
CBAM	Mat/sheet with randomly oriented short fibers [97]		Carbon fiber/ Kevlar/ fiber glass/ high-density polyethylene	165	-	-	[45]
SLS		Nano	CNT (0.5 wt %)/PA-12 & PU	-	-	Thermal conductivity: up to 16.9 W m^{-1} K^{-1}	[41]
	Discontinuous		Carbon black (4 wt%)/PA-12	26	1.0	Flexural modulus: 1.4 GPa Flexural strength at 5% strain: 65 MPa Impact strength: 12 J/m	
			Carbon nanofiber (3 wt %)/PA-12	-	-	Storage modulus at room temperature: 1.2 GPa	[42]
		Micro	YSZ (5 wt%)/ PA-6	25	-	-	[101]
			Glass beads (30 vol%)/PA-11	-	1.7	Near full density of 99% Compressive modulus: 2.6 GPa	[102]
			SiC (10,25,50 wt %)/PA-12	34-40.5		Reduced strength with higher loading High porosity: >20%	[105]
			Nanosilica (3 wt%)/PA-12	20.83	1.98	Impact strength=40.2KJ/m2	[106]
			Glass fiber (25 wt%)/PA-12	43.7	2.71	Fracture properties K_{IC}: 3.9 MPa·$m^{1/2}$	[109]
			carbon fibers (100-200 μm) / PA-12	-	6.3	V_{xy}: 0.443 V_{xz}: 0.383	[120]
				-	3.54	V_{yx}: 0.225	

	-	2.96	V_{yz}: 0.479 V_{zx}: 0.163 V_{zy}: 0.388	
Carbon fiber(150–250 μm) (30wt%) / PA-12	72	5.5	Flexural strength: 106 MPa Flexural modulus: 5.3 GPa	[121]
thermally and HNO_3 treated Carbon fiber (150–250 μm)(30wt%) / PA-12	80	5.8	Flexural strength: 114 MPa Flexural modulus: 5.9 GPa	[121]
Glass fiber (99 μm) (30 wt%)/ cPBT	60	-	Flexural strength: 90 MPa Impact strength: 2 kJ/m^2	
wollastonite fibers (20–80 μm)(25 wt%)/ PA-12	40	3.6	Flexural creep modulus: 3.6 GPa	[122]
Glass fiber (75 μm)/ Polystyrene	-	-	Flexural strength: 16.34 MPa	[107]
Glass fiber (10 wt%)(50 μm) / poly(propylene-co-ethylene)	19.3	0.775		[123]
Glass fiber (20 wt%)(50 μm) / poly(propylene-co-ethylene)	17	0.9		
Glass fiber (30 wt%)(50 μm) / poly(propylene-co-ethylene)	15.7	1.15		

3. Future Outlook

AM processes for FRPC are contributing to revolution in various fields. This section discusses the past research work that has been done in specific topics such as materials development, composition and homogeneity, porosity, fiber matrix interface, fiber alignment, and interlayer bonding, as well as some new developments and future possibilities, which will spark new research in this field. With respect to this, as there are limited studies on the AM of composite materials, relevant works for AM pure polymers and non-AM composites are taken into discussion when necessary as they can be expanded for the use of AM of composite materials.

Material development

AM polymeric materials with limited mechanical strength and durability by nature have been incorporated with reinforcement to form composites with improved performance in these aspects and as well as enhanced thermal, optical and electrical properties to be used in various industries. Particularly these reinforced composite materials have been created for uses in aerospace, automotive, and wind energy industries and other industries that demand materials with high mechanical performance. Fibers of various forms (short, continuous, sheet) and scales (nano, microns, mm, cm) have been used to form composite materials for different AM techniques.

Research on the short fiber reinforcements make up more than 80% of the research work on the AM composite materials. This is probably due to the ease in the preparation of the short FRP composite materials and the technological limitations that hinder the use of other form of reinforcements such as continuous fiber and fiber sheet. The need for higher stronger materials for AM have led to the development of various AM-friendly continuous FRP composites. Most commonly used continuous reinforcements are carbon fibers, glass fiber and Kevlar fiber. As

shown in the table 2, continuous fibers are able to provide higher tensile properties as comparted to the short fibers.

Despite the rapid growth in the AM technology, current systems still rely on narrow range of commercial and proprietary resins, thus limiting the physical and chemical properties of parts [17]. While most of the current research aims for enhancing the mechanical performance, there has been increased interest in developing functionalized materials with broader range of properties, such as thermal [58], piezoelectric [30], electrically conductivity [18, 41], dielectricity for radio frequency or microwave applications [20, 124, 125], and for biomedical applications [126]. AM FRPC also enables the fabrication of functionally graded structures by controlling the spatial distribution of composite to produce localized control of specific properties. For example different arrangement of materials with different permittivity can produce diverse resonant frequencies [124] and different localized refractive indices [20]. Yang et al. fabricated a double-layer laminate smart material which consists of CF/PEEK , which can change shape due to the mismatch in strain between the surface layer and the basal layer through electrical heating [21]. Continuous wire polymer composites using extrusion technique is being developed to produce thermal and mechanical sensors and to fabricate heating elements integrated into AM structures [19].

The research on AM composite materials is not restricted to the above-mentioned AM techniques. For instance, multi-material AM process, namely the multi-material jetting process, has the capability to fabricate composite by selectively depositing two or more different materials at the designated location. This unique characteristic enables a new design paradigm of creating FRPC using multi-material AM, thus pushing the boundaries and definition of FRPC. Instead of using actual fibers as reinforcement, the fibers can be printed in milli-scale using a stiffer ink to reinforce a softer matrix ink [127]. The fiber/matrix composition and orientation can also be spatially controlled. Their geometry, for instance, the fiber shape and

dimension, can be varied without any manufacturing restrictions, during the design stage.

Recent research has revealed several emerging applications of multi-material AM FRPC such as soft robotics [128], biologically inspired materials [129], medical phantom models [130], and even 4D printing [131]. Varying complex fiber configurations based on the requirements of targeted application can hence be produced without the need of process modification or material formulation.

Multi-material AM process has enabled the fabrication of sandwich composite. Sandwich cores, such as lattices [132], honeycombs [133] and other cellular structures [134, 135]; and honeycomb sandwich made by adhesively assembling sandwich core to additively manufactured FRP facesheets [135] have been produced successfully using AM. The creation of hybrid one-step process that allows the fabrication of functional composite with integrated structures would disrupt the current composite industry and design paradigm.

Fiber-matrix interfacial properties

The properties of composite materials are affected not only by the properties of the individual parent materials but also on the morphology and interfacial characteristics. The fiber-matrix interfacial shear stress is an important parameter that controls the effectiveness of stress transfer and determines the off-axis strength and impact toughness of CFRP, environmental stability of CFRP and functional performance of CFRP [136]. The interfacial properties can be controlled by changing the composition, structure and distribution of the interface [137].

In AM field, the research on the interface of the composite is still not comprehensive as most of the research is still focused on the characterization of the mechanical properties of the bulk composite materials as shown in table 2. Research on the characterization of the interfacial properties of the composite materials fabricated using AM techniques is not well studied. In most studies, the interfacial properties were deduced qualitatively from the SEM images [38, 52]. More detailed research to evaluate the interfacial strength of composites in three different levels

such as macroscopic test methods, mesoscopic interface test methods and micro-composite

experimental methods should be conducted for 3D printed composites [138]. Macroscopic test methods are adopted to assess the interfacial adhesion between fibers and polymer matrix at the macro-scale. However, macroscopic tests are meant for qualitative comparison of the interfacial bonding properties, not for the independent quantitative estimation of the interfacial strength. To author's knowledge, no quantitative characterization was performed to investigate the fiber-matrix interfacial properties of the additively manufactured composite materials. Moreover, the fast heating and cooling nature of 3D printing processes, which differ from conventional composite manufacturing techniques, certainly warrants further investigation on how the mechanisms at the interfacial level work. For instance, nanomechanical interlocking, thermal residual stress due to mismatch in coefficient of thermal expansion[139], non-binding energy and sliding frictional stress [140] are a few the mechanical interactions at the interface that should be investigated in detail in order to have a better understanding of how the fiber-matrix interface affects the final mechanical properties.

Also, it is well known that unmodified fibers, especially carbon fiber, have smooth fiber surface that lacks active groups to interact with polymer matrix. Hence, modification on the interface should be performed, which are normally accomplished by enhancing the surface polarity of fiber, improving the wettability between fiber and polymer, and also stimulating the chemical reaction. The interfacial modification methods have been well developed for non-AM fiber reinforced composites and have been critically reviewed [141]. However, thus far, studies on fiber surface modification and use of coupling agent in AM composite materials are mostly done for SLS [121, 123, 142] SLA[143] , and FFF [52, 144] techniques and are focused on the improvement of mechanical properties. Oxidation modification method through nitric acid treatment has been used to improve the fiber-matrix interfacial properties in SLS PA12 based composite materials [121, 142]. This treatment removes the impurity on the fiber surface, which

prevents the formation of weak interfacial bonds, and etches the fiber surface to increase the surface area and roughness, which improves the physical interlocking. Apart from that, oxygen functional groups (C–O, C=O and O–C=O) are introduced and the concentration of O element is improved as the result of the modification, which improves the interfacial adhesion between the fibers and the nylon matrix through the hydrogen bonding between oxygen functional groups (CO, CO and OCO) on carbon fibers and the amide bonds in PA12. However, the introduction of these oxygen functional groups poses porosity issue which arises from the gas accumulation within the composite materials due to the thermal decomposition of oxygen groups during the laser sintering process[145]. Thermal treatment in inert atmosphere has found to be effective in selectively reducing the oxygen groups while retaining the interface compatibility[121]. The carbon nanotube surface has also been functionalized using potassium permanganate as the oxidant. The functionalized carbon nanotube can form –NHCOO– and –NHCO– bonds with the toluene diisocyanate (TDI) in the in-situ polymerization process in SLA [143]. For natural fibers (such as spruce thermomechanical pulp (TMP)) that are normally hydrophilic in nature, surface modification was done via enzymatic treatment to improve their compatibility with the hydrophobic resin[144, 146]. The laccase-mediated grafting of octyl gallate onto TMP fibers improved their interfacial adhesion with PLA by oxidizing and removing lipophilic extractives from the TMP fiber surface [144]. Apart from that, laccase can graft some hydrophobic compounds onto the natural fiber surfaces to reduce the water take up of the fiber[147]. Apart from PLA, this method has been used in polypropylene[146, 148] and epoxy-based [149] composites. In another study, coupling agent based on polypropylene grafted with maleic anhydride was used to promote adhesion between the glass fiber and the polypropylene matrix [123]. To authors' knowledge, there has not been any study that focuses on the surface modification of carbon fiber for composite materials used in FFF and LOM and how the surface properties affects other material properties such as electrical and optical properties. Therefore,

there is a need to have more in-depth investigation on the fiber-matrix interface of AM composite materials in order to achieve desired mechanical, electrical or optical properties of the composite parts.

Fiber homogeneity

Homogeneity of the fiber distribution is important to ensure efficient transfer of stress from the matrix to the reinforcements. It is evident from the results from a few groups that the strengthening effect is more obvious in lower fiber loading and diminishes and even deteriorates at high fiber loading especially for short fiber reinforcements [23]. The drop in strength is probably due to the poor stress transfer from matrix to fibers which caused by inhomogeneity of the composite materials. Tekinalp et al. also reported that the standard deviation of the results for the composite material is significantly higher than that of the pure thermoplastics materials and attributed it to the sample-to-sample differences in the fiber distribution [23]. It is therefore important to ensure the homogeneity of the composite material. Mixing methods used to produce the composite materials varies with fabrication techniques and are discussed in detail.

In FFF, to ensure homogeneous fiber dispersion, the nylon pellets are first ground to a particle size of approximately 200-500 μm [56]. Surfactant is coated on the iron reinforcement to improve the dispersion by lowering the high free energy surface of iron fillers. The coated iron particles can provide good link to the lower free energy surfaces of polymer particles. The nylon and iron reinforcement were mixed in a tumble mixer for 2 hours to produce the homogeneously mixed composite material.

Gray et al. used a dual extrusion process to spin self-reinforced Thermotropic liquid crystalline Polymers(TLCP) /PP composite strands [50]. The TLCP was injected into the PP matrix (which is at 245 ^{o}C) as continuous streams at 325 ^{o}C. The melt was then extruded through a capillary

die with a diameter of 1.8 mm to form the composite strands. The composite strands were then hot-pressed at 180^{o}C into plaques. The strands, which were cut into length of 6 cm, were mixed randomly into a preheated mold to be consolidated with 1 MPa of pressure. The plagues were granulated to form granules with 6.3 mm diameters. The granules were then fed into a single screw extruder (which operates at 177^{o}C and 10RPM) to produce the composite filament.

For AM techniques such as LDM and SLA that use liquid or paste based feedstock, the method for preparing the composite materials are similar, which is by mechanical stirring and ultrasonication. In LDM, homogenous composite material is prepared by first dissolving 3wt% of PLA in DCM by magnetic stirring at room temperature for 3 hours [73]. MWCNTs reinforcement is added in the PLA/DCM solution to form the composite feedstock material by magnetic stirring at 950 RPM for 30 minutes and followed by 1 hour of ultrasonic bath at room temperature and lastly 30 minutes ultrasonication. Ultrasonication is known to have negative effect on the fiber structure such as reducing the fiber length especially in low viscosity solution[150]. In SLA, nano-carbon black were stirred with the liquid resin which contains tetra function polyester acrylate and 1,6-Hexanediol di-acrylate for 24 hours at 1000 rpm to form the homogeneous composite material [81]. Dispersant (TEGO dispers 680 UV) was also added to prevent agglomeration of nano-carbon black. In another study using LDM, acid treatment was performed on MWNTs to ensure uniform dispersion of of the CNTs in aqueous solution [76]. The acid treatment introduces functional group such as carboxylic acid and hydroxyl groups on the MWNT surface which improves the ionic character of the nanotubes.

In SLS, in which composite materials exist in powder form, various methods have been used to produce homogenous composite feedstocks, such as melt mixing[42], mechanical mixing[151], and dissolution precipitation. In melt mixing method, the polymer powder is first dried to prevent hydrolytic degradation during the process [42]. The dried polymer powder and the carbon nanofiber were mixed at 190 ^{o}C for 10 minutes at 60 rpm using a mixing equipment.

After mixing, the homogeneously mixed composite material was compression molded and cryogenically fractured to produce composite powders with average particle size of 50 μm. In pure mechanical mixing of thermoplastic powder and reinforcement, the fibers were sieved through a 1 mm mesh size sieve to ensure that the mixed composite feedstock material is processable in SLS [151]. The fibers were then mixed with the thermoplastic powder in a mixer for 10 minutes. In dissolution precipitation method, the nanoparticle reinforcement is first mixed with a solvent, that comprises of 95wt% ethanol, 4.5wt% butanone, and 0.5wt% distilled water, by agitation, and further treated with ultrasonic oscillation at 30^{o}C for 2 hours to form a nanosilica emulsion [106]. The PA12 pellet is dissolved in to nanosilica emulsion. The emulsion that contains dissolved PA12 and nanoslica is then put into a N_2-filled reactor. In the reactor, the emulsion is then heated up to 145^{o}C to resolve PA12 thorougly and cooled at a rate of 10^{o}C/hour to 105^{o}C to let PA12 to precipitate. Vacuum drying and ball milling were performed on the precipitation to obtain the nanosilica/PA12 composite powder.

Although various methods of mixing have been developed, there seems to be lacking quantitative checks on the homogeneity of the fiber distribution for all material production techniques. Absorbance intensity has been used as a measure to quantify the dispersion of the CNTs in LDM [152]. However, this technique is only suitable for composite material where there is distinctive difference in optical absorbance at a specific wavelength between the reinforcement material and the matrix material. Techniques such as in-situ monitoring of the mixing process could potentially help improve the quality of the feedstock materials.

Fiber alignment

The coordinated arrangement of short and continuous fibers within the additive manufactured composites is currently being researched on. Typically, in material extrusion processes, it is found that initially the fibers are not fully aligned in the composite filament, but shearing force between fibers and nozzle walls give rise to alignment during the AM process [29, 52]. The

phenomenon is also captured in the simulations of the extrusion of short FRPC by two different groups, Lewicki et al.[153] and Yang et al. [154]. Simulation results suggested that internal surface to volume ratio of the nozzle and rheology properties of the continuous phase fluid are two important factors to achieve efficient shear alignment in extrusion. Yang et al. noted that the fiber alignment of the deposited composite materials is affected by the flow split that occurs outside of the nozzle which will result in a much more complex velocity contour of resin flow. In the same study, the extrusion of continuous fiber through a nozzle is also simulated. However, the model only considered single strand fiber.

In SLA, Shear induced alignment has been recently demonstrated using linear oscillatory actuation mechanism combined with the SLA process [155]. A number of other new techniques employed to manipulate the fibers in the resin include use of magnetic [34, 156], electric [32] and acoustic fields [36, 157]. The developments of these new methods have pointed out the importance of aligned fibers in the AM of FRPC.

Additive manufacturing enables the precise control of the fiber's alignment within a layer in the polymeric matrix, allowing the variation of mechanical properties such as stiffness and toughness and thermal properties [58] within design components to satisfy specific design requirement. For instance, the effect of different fiber layup patterns on mechanical properties have been investigated by various research groups. Isotropic fiber layup generally provides better tensile strength than concentric fiber layup of the same fiber volume fraction [158]. Also, 0^o fiber orientation has the best tensile strength whereas 90^o fiber orientation has the weakest tensile strength [116, 159]. These studies have shown the importance of fiber alignment as the strength comes in the fiber direction. In one study, epoxy-based matrix composite material that contains silicon carbide (SIC) whiskers and carbon fibers were used in the attempt of using AM technique to create a network of repeating cell units [29]. By controlling the fibers alignment within the composite, hierarchical honeycomb structures that mimics the natural balsa wood

was fabricated. This method demonstrates the ability for the creation of different bio-inspired composite objects with precise architecture and mechanical properties. Moreover, controlling fiber alignment also enables creation of atmosphere-sensitive composites. For example, hygromorphic biocomposites that are capable of bending in response to a moisture gradient was been created to by using AM materials with natural fibers [160].

Interlayer bonding

As additive manufacturing is a layer by layer process, the bonding between the adjacent layers becomes an important factor in determining the strength of the resulting printed parts, especially in the z-direction. The research on the interlayer bonding of the AM of pure thermoplastics has been performed [161]. In generally, parameters such as z-direction tensile strength, mode I interlaminar fracture toughness [162] and interlaminar shear strength [113, 163] have been used to gauge the interlayer properties. In general, the z-direction tensile properties are weaker than that of the in-plane tensile properties as observed from various AM techniques such as FFF [163], SLS [164], and inkjet [165]. In polyjet, the ultimate tensile strength in the z-direction is only 60% of that of the UTS in x and y-directions [165]. In SLS, the fracture strain in z-direction found to be lower than that of the x-direction, indicating the interlayer fracture is more brittle than intralayer fracture [164]. This shows the importance of the effort to improve the interlayer bonding of AM materials.

In FFF, it is found that printing parameters such as higher nozzle temperature, higher bed temperature, smaller layer thickness, lower printing speed enhances the interlayer bonding [166]. Aliheidari et al. found that increasing nozzle temperature from 210 ^{o}C to 240 ^{o}C would enhance the mode I fracture toughness from 2167 to 3907 J/m^2 [162].This is because higher average temperature and lower printing speed would result in the deposited materials having a longer

time staying above the glass transition temperature, favoring the bond formation between the layers.

The interlayer properties of the FFF-fabricated pure polymer have been compared with that of the polymers fabricated using conventional processes. The mode I interlayer fracture toughness (1.57 kJ/m^2) of the was found to be 4 times lower than that of the compression molded polymer parts (6.11 kJ/m^2) [167]. Apart from that, the effect of the addition of reinforcements to the polymers on the interlayer properties has been investigated. All studies have shown that the interlayer properties drop with the addition of the fibre reinforcements. For instance, the Z-direction tensile properties of the carbon fiber-filled ABS is only 7 MPa or 42% of that of the pure ABS (16.75 MPa) [22]. Apart from that, another study has shown that the interlayer fracture toughness of the carbon fiber-filled ABS (0.33 kJ/m^2) is about 5 times lower than that of the pure ABS (1.57 kJ/m^2) [167]. Another study showed that the interlaminar shear strength of the reinforced ABS is 8.5 times lower than that of the pure ABS [27]. This suggests that the strengthening of the in-plane properties by the addition of reinforcement comes at the expense of poorer interlayer properties. This is because the addition of reinforcement reduces the amount of bond formation of the thermoplastics at the interlayer boundary. Other possible reason for the lower interlaminar shear strength of composite materials could be due to the higher thermal conductivity of the fiber as compared to the polymer matrix [168] which leads to higher cooling rate and in turn reducing the time for bond formations. Printing parameters are found to have effects on the interlaminar properties. Zhang et al. saw a drop in shear strength from 13 to 10.5 MPa when print speed was increased from 60 mm/s to 100 mm/s and layer thickness from 0.18mm to 0.3 mm. Although some work to improve the interlaminar properties of FFF-fabricated materials has been going on such as in-process pre-deposition laser heating [169], adding CNTs, using microwave irradiation [170] and controlling the chamber temperature [171], the improvement of the interlayer properties is not significant. It could be attributed to the

lack of consolidation process that stimulate the mobility and diffusion of the polymer chains.

To overcome this, Parandoush et al. incorporated compaction roller and a laser source in attempt to enhance the interlaminar lap shear strength through pressure and heat [172]. It was found that by using a laser power of 26W and roller speed of 1~2 mm/s, the lap shear strength obtained was 96% of that of compression molded specimen (9.87 MPa). However, the effect of the compaction force was not investigated in their study.

It has been established earlier that interlayer fusion bond plays a major role in the z-direction tensile strength. However, improving the interlayer bonding alone is not sufficient to achieve superior z-direction tensile strength comparable to the in-plane tensile strength. This is due to the nature of AM involving layer-by-layer fabrication where the reinforcement fibers can only be laid in-plane. Delamination is likely to occur without the through-thickness fibers, resulting in anisotropic properties. Traditionally fiber stitching, braiding, weaving, and mechanical insertion of out-of-plane fibers are used to improve the inter-laminar properties. Quan, Wu, Keefe, Qin, Yu, Suhr, Byun, Kim and Chou [173] presented the capability to design and fabricate multi-directional reinforced composites like the 3D through-thickness interlock woven structures and 3D braided structures using FFF. The multi-directional fibers, however, are printed layer-by-layer to form the structures, and the through-thickness fibers are still subjected to the anisotropic effect of AM. There is, hence, a need to develop new methods to produce through-thickness reinforcements by multi-axis fiber laying to overcome severe anisotropic properties of the AM processed FRPC.

Porosity

Pores and voids refer to spaces that are supposed to be filled but not filled with materials. The presence of voids reduces the material integrity of the parts which results in poorer mechanical properties. Hence, it is important to know the causes of the pore formations so that they can be reduced if not eliminated.

There are several factors that can lead to the presence of voids in the printed parts. Some voids are inherently present even without the addition of fiber into the polymer matrix. The formation of these voids is due to the nature of the fabrication process. For instance, triangular voids are commonly found between the adjacent filament in the FFF-fabricated parts. These voids can be minimized by reducing the distance between the adjacent filament. The technique-induced pores were also found in SLS printed parts where pores are aligned along the layer orientation (coplanar) which results in the anisotropic characteristics of the SLS-fabricated parts [174].

In SLS, printing parameters play important roles in the resulting porosity. Laser power, beam speed and scan spacing which affect the energy density are found to have effect on the porosity and the tensile strength of the SLS-fabricated parts [105]. Proper fusion would not occur among the thermoplastic matrix powder if the energy density is too low, which happens at low laser power, high beam speed and large scan spacing, resulting in increased porosity. Too high the energy density, on the contrary, would result in degradation of polymer, which would also lead to higher porosity. Hence, proper selection of printing parameter is required to achieve a minimum porosity level.

Apart from technique-induced porosity, porosity can arise from the condition the thermoplastic matrix. For instance, in FFF, it was found out that although the raw composite filament, which was fed into the heated nozzle, did not exhibit significant porosity, the extruded composite was found to have porosity in the range of 20-30% [175]. It was found that the porosity was the result of the volume expansion of the moisture in the thermoplastics as well as the gas generated due to the degradation of the thermoplastics due to the extreme temperature condition at the nozzle. Hence, proper storage of the thermoplastic is usually required to keep the composite material in dry state.

In a study by Tekinalp et al. [23], it was found that the addition of fibers would cause a change in the type of pore formation. At lower fiber content, the larger triangular voids between the

adjacent filament is more dominant. As fiber content increases, the triangular voids become smaller due to better packing of the deposited filament, which is the result of decrease in die swell due to increase in thermal conductivity with the addition of carbon fiber. However, another type of voids, which is the smaller-sized voids inside the extruded filament, becomes dominant. These smaller-sized voids are found around the fibers-matrix interface and is a result of partially independent flow during the extrusion process of FFF due to the incompatibility between the two phases. Hence, surface treatment of fiber is necessary to reduce the formation of the inner-filament porosity. The compression molded composite parts were also fabricated to serve as a comparison with the FFF-fabricated parts. It is found that the FFF-fabricated parts exhibit significantly higher porosity as compared to the compression molded parts. The higher porosity could also be attributed to the lack of consolidation during the fabrication process. Similar finding has been reported by Wu et al. for SLS printed parts[121].

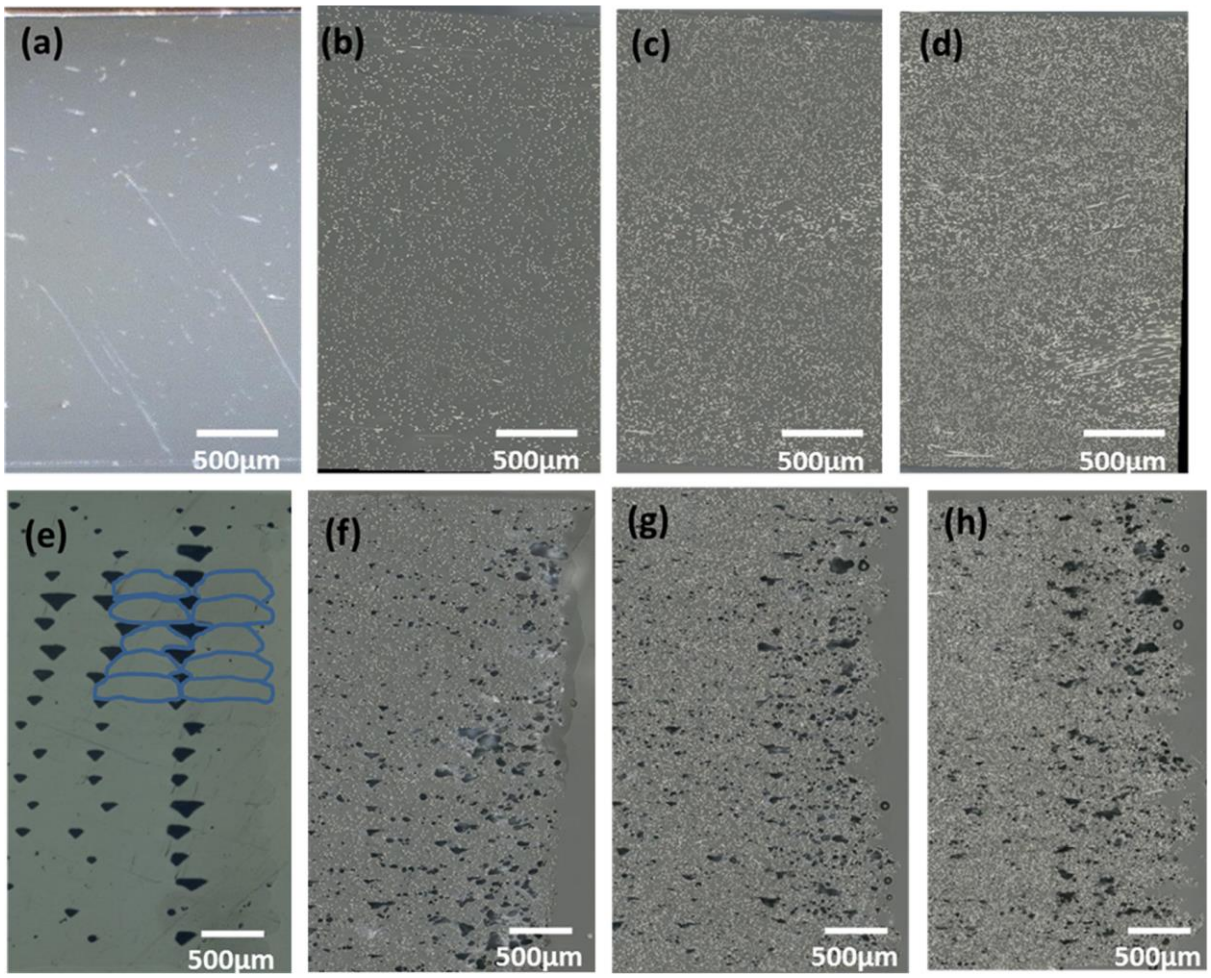

Figure 7. Fracture surface SEM micrographs of (a) and (b) neat-ABS fused deposition modeling (FDM)-printed, (c) 10 wt% carbon fiber-loaded FDM-printed, and (d) 10 wt% CFloaded [23]

In comparison with the FFF and SLS, LOM performs better in terms of porosity. Klosterman et al. [44] managed to achieve porosity as low as 5% using post-LOM consolidation process. This shows the importance of having in-process consolidation process for the AM techniques when fabricating composite parts.

Printability Issue

Addition of reinforcement changes the rheology of the material which introduces printability issues that can be either beneficial or detrimental to the AM techniques. Careful control of the rheology response is therefore required when formulating the 3D printable composite materials.

Viscosity is the most commonly investigated material properties in extrusion based technique[176, 177, 178, 179], vat photopolymerization technique [90, 91, 180, 181] and the powder bed fusion technique [182, 183]. The viscosity requirement for each type of technique varies. In extrusion-based AM technique, low viscosity fluid ink is not suitable for the fabrication of 3D structures [179]. This is because the ink and lacks self-supportability and shape retention ability. The ink viscosity suitable for 3D printing is reported to be in the range of 10^1 to 10^3 Pa.s [178]. Specifically in LDM, the viscosity of composite feedstock existing in aqueous solution is normally too low for good extrusion and would require thickener to improve printability. On the other hand, nozzle clogging issue will arise in extrusion-based AM technique if the viscosity is too high. This phenomenon commonly happens in FFF technique in which the molten pure thermoplastics themselves have high viscosities and adding reinforcement would shift the rheological behavior out of the processing window of FFF. Wang et al. provided a guideline of using melt flow index (MFI) to check the printability of the material in FFF without going into the detail on the rheology of the material [181]. They found out that a minimum MFI value of of 10 g(10 min)$^{-1}$ at 2.16kg is needed to have a successful extrusion in FFF.

In SLA, rheology plays a part during the coating of the new layer. Typical range of viscosity is between 0.1 to 100 Pa.s[91, 180, 184] for materials used in SLA, although viscosity as high as 500 Pa.s [185] has also been successfully coated by doctor blade into a thin layer. For bottom-up SLA technique, the viscosity should not be higher than 0.5 Pa.s as resin would not have sufficient time to fill in the new layer gap when the platform is raised, thus causing fabrication failure [180]. In the melt rheology study of SLS material, the zero-shear viscosity is the parameter of interest since no shear flow applied [182]. Low Zero-shear viscosity is beneficial for coalescence of during the sintering.

Similar to other AM composite materials, the viscosity of the composites increases with the addition of CNT loading. The increase in viscosity was due to interaction between the

reinforcement and thermoplastic hindering the movement of the polymer chains [183]. Addition of the fiber changes the rheological behavior of the pure SLA resin from being a Newtonian fluid into shear thinning [90, 91, 180]. Fiber length have considerable effect on the viscosity at low shear rate. For instance, viscosity increases by a factor of ten when the length of the glass fiber increases from 0.8mm to 1.6mm[90]. Lozano et al. reported that the viscosity change is negligible for the concentration below 10wt% of VGCFs but increases sharply just below the maximum packing fraction [186]. As VGCF/PP exhibits shear-thinning behavior, the high viscosity composite material due to higher reinforcement concentration can be compensated by higher extrusion rate.

Rheology modifiers are normally added to control the viscosity so that the composite material is printable. For instance, PVP, which is a hydrophilic water-soluble polymer, is used in LDM to increase the viscosity of the aqueous-based CNT ink. The PVP was non-covalently wrapped onto the CNT to improve the steric stabilization of the CNT via the resultant presence of hydrophilic chains on the CNT surface [176]. The viscosity of the ink can be controlled by the varying the amount of PVP in the solution. However, non covalent solution technique poses some problems: degradation of CNTs and limitations of popular surfactant such as sodium doecyl sulfate (SDS) on the CNTs concentration [177].

Apart from melt rheology, powder flowability is another property that affect the processability of the composite materials. Particles size affects the feeding quality of the powder layer using roller mechanism. Extremely fine powder (size less than 10 μm) would also cause processability issue due to higher interparticle friction[187]. Larger powder would cause the layer surface to be course. Particle size in the range of 10-100 μm is found to be suitable for SLS technique[188]. Fibers with high aspect ratio can reduce the flowability. Flowability decreases with the increase in fiber loading. Lubricating agent such as calcium stearate was used to reduce the interparticle friction and thus improving the flowability. Fiber loading of up

to 50% was achievable in carbon fiber/polyamide composite system with the help of the lubricating agent [142].

Modeling, Simulation and Topology Optimization

Physics-based modelling and simulation are important not only to predict the outcome of the AM process on FRPC, but also to allow prediction of additively manufactured composite part's performance at the design stage. The modeling approaches to various AM techniques have been critically reviewed by Bikas et al. [189]. In FFF, critical reviews of the extrusion process have been done which are focused on the physics of the process [190] and the accuracy and surface roughness of the FFF-fabricated parts [46]. In addition, the parametric process model was developed to estimate the energy consumption and the environmental impact [191]. In SLS, the thermal analysis methods for the powder bed fusion technique have been reviewed [192]. In LOM, the mathematical model and simulations of LOM to study the process parameters[193], thermal effect [194]and cure distribution [195] have been developed. Apart from that, topology optimization, which optimizes the material distribution for best part performance, has been widely used in the design of additively manufactured parts [196]. Current modellings, simulation of AM processes and topology optimization algorithm are developed mostly for single material [197]. Addition of fiber reinforcement introduces several more parameters such as the composition of composite materials, distribution, alignment of fibers and anisotropy of thermal conductivity of continuous FRP composite which should be considered when developing new models for AM process on FRPC to assure the quality and performance of the additive manufactured FRPC. For instance, the in-plane thermal conductivities of the composite materials have been known to be almost 10 times higher as compared to the through-the-thickness thermal conductivities[198]. This anisotropy would significantly change the way heat is being dissipated from the deposited composite materials and in turn affecting the thermal history for interlayer bonding which certainly warrants further investigation.

Large Format Composite Printing

Low productivity is one of the key technological barriers in adopting AM for commercialization. Developing techniques that can synchronize multiple robots for faster processing using the materials that are scalable can enhance productivity. Incorporation of extrusion head with multi-axis robotic arm will also expand the manufacturing scale and flexibility by providing additional degree of freedom to print the FRPC [97]. An extrusion-based printing with a six-axis robotic system has been developed to achieve a scalable and efficient platform for FRPC [199]. Another large format printing for FRPC is selective lamination composite object manufacturing (SLCOM), which is a combination of inkjet and LOM processes with ultrasonic cutter. This technique forms FRPC using traditional prepregs like woven reinforcement of Kevlar, carbon and glass fibers, which are impregnated with thermoplastic matrix [200].

4. Conclusion

This progress report has summarized recent efforts on the material developments for AM processes, advancement in various AM processes, and resulting mechanical and other functional properties of AM-fabricated FRPC. The addition of reinforcement into the polymers has improved the mechanical properties and widened the functionality of the polymers. Generally, the ultimate performance of the continuous FRPC are potentially more outstanding compared to the discontinuous FRPC as has been already demonstrated by many studies.

FFF, LDM, stereolithography, LOM, CBAM, and SLS have their own special features and advantages in fabricating FRPC with ultimate mechanical and functional properties. Majoy problems are related to processability of the materials, interfacial properties and the interlayer properties of the AM-fabricated FRPC. Selecting the appropriate AM technique and finding

proper binder is crucial for achieving the best mechanical performance as well as other non-

mechanical properties.

In conclusion, the best performing FRPC shown in table 2 in terms of tensile strength are compared with FRPC fabricated using conventional fabrication techniques as shown in fig 3. In the figure, regions of different colors correspond to tensile properties of different fabrication techniques available in literature.

The figure shows some best results reported to date for various AM processes. Two observations can be made; 1) short fiber reinforced polymer composites (regardless of which technique used) perform poorer in term of tensile strength as compared to composites fabricated using conventional techniques. 2) Although FFF and LOM can produce composites with relatively good strengths (500-800MPa), they still fall short in comparison to the tensile strength (up to 1500 MPa) and fiber loading (up to 70%) of the conventionally manufactured composites. This leaves exciting opportunities for the various methods to further enhance the mechanical properties of the FRPC to be explored in the near future through material development and process enhancement with the help of physic based modeling and simulation.

Acknowledgements

This work was supported under the grant by National Research Foundation (NRF).

References

[1] M. A. Abanilla, Y. Li, V. M. Karbhari, Composites Part B: Engineering 2006, 37, 200; M. A. Abanilla, V. M. Karbhari, Y. Li, Composites Part B: Engineering 2006, 37, 650; Y. Wang, Applied Composite Materials 2002, 9, 81.

[2] Y. Wang, Applied Composite Materials 1999, 6, 19.

[3] D. A. Papargyris, R. Day, A. Nesbitt, D. Bakavos, Composites Science and Technology 2008, 68, 1854; D. Abraham, S. Matthews, R. McIlhagger, Composites Part A: Applied Science and Manufacturing 1998, 29, 795; Y. Zhou, F. Pervin, S. Jeelani, P. K. Mallick, Journal of materials processing technology 2008, 198, 445.

[4] R. Luchoo, L. T. Harper, M. D. Bond, N. A. Warrior, A. Dodworth, Plastics, Rubber and Composites 2013, 39, 216; L. Harper, T. Turner, J. Martin, N. Warrior, Journal of composite materials 2009, 44, 931; A. Ionita, Y. J. Weitsman, Composites science and technology 2006, 66, 2566.

[5] H. J. A. L. Dirk, C. Ward, K. D. Potter, Composites Part B: Engineering 2012, 43, 997.
[6] K. Croft, L. Lessard, D. Pasini, M. Hojjati, J. Chen, A. Yousefpour, Composites Part A: Applied Science and Manufacturing 2011, 42, 484.
[7] F. Abdalla, S. Mutasher, Y. Khalid, S. Sapuan, A. Hamouda, B. Sahari, M. Hamdan, Materials & design 2007, 28, 234.
[8] C. C. M. Ma, C. T. Lee, H. D. Wu, Journal of applied polymer science 1998, 69, 1129; C. H. Chen, C. C. M. Ma, Composites science and technology 1994, 52, 427.
[9] C. K. Chua, K. F. Leong, *3D Printing and Additive Manufacturing: Principles and Applications Fifth Edition of Rapid Prototyping 5th Edition*, World Scientific Publishing Co., Inc., 2017.
[10] R. Dermanaki Farahani, M. Dubé, Advanced Engineering Materials 2018, 20, 1700539.
[11] B. Brenken, E. Barocio, A. Favaloro, V. Kunc, R. B. Pipes, Additive Manufacturing 2018, 21, 1.
[12] P. Parandoush, D. Lin, Composite Structures 2017, 182, 36.
[13] S. Kumar, J. P. Kruth, Materials & Design 2010, 31, 850.
[14] Z. Quan, A. Wu, M. Keefe, X. Qin, J. Yu, J. Suhr, J. H. Byun, B. S. Kim, T. W. Chou, Materials Today 2015, 18, 503.
[15] X. Wang, M. Jiang, Z. Zhou, J. Gou, D. Hui, Composites Part B: Engineering 2016, 110, 442.
[16] J. Cerneels, A. Voet, J. Ivens, J.-P. Kruth, "Additive manufacturing of thermoplastic composites", presented at *Composites Week@ Leuven*, 2013; N. Mohan, P. Senthil, S. Vinodh, N. Jayanth, Virtual and Physical Prototyping 2017, 12, 47; T. Hofstätter, D. B. Pedersen, G. Tosello, H. N. Hansen, Journal of Reinforced Plastics and Composites 2017, 36, 1061; J. Frketic, T. Dickens, S. Ramakrishnan, Additive Manufacturing 2017, 14, 69.
[17] U. Kalsoom, P. N. Nesterenko, B. Paull, RSC Advances 2016, 6, 60355.
[18] M. Saari, B. Cox, E. Richer, P. S. Krueger, A. L. Cohen, 3D Printing and Additive Manufacturing 2015, 2, 32.
[19] Y. Ibrahim, G. W. Melenka, R. Kempers, Manufacturing Letters 2018, 16, 49.
[20] A. R. David, L. G. Brandon, M. Raymond, Y. Shridhar, S. Jared, G. Austin, P. Peter, S. M. Mark, Smart Materials and Structures 2014, 23, 045029.
[21] C. Yang, B. Wang, D. Li, X. Tian, Virtual and Physical Prototyping 2017, 12, 69.
[22] L. J. Love, V. Kunc, O. Rios, C. E. Duty, A. M. Elliott, B. K. Post, R. J. Smith, C. A. Blue, Journal of Materials Research 2014, 29, 1893.
[23] H. L. Tekinalp, V. Kunc, G. M. Velez-Garcia, C. E. Duty, L. J. Love, A. K. Naskar, C. A. Blue, S. Ozcan, Composites Science and Technology 2014, 105, 144.
[24] M. L. Shofner, K. Lozano, F. J. Rodríguez-Macías, E. V. Barrera, Journal of applied polymer science 2003, 89, 3081.
[25] M. L. Shofner, F. J. Rodríguez-Macías, R. Vaidyanathan, E. V. Barrera, Composites Part A: Applied Science and Manufacturing 2003, 34, 1207.
[26] F. Van Der Klift, Y. Koga, A. Todoroki, M. Ueda, Y. Hirano, R. Matsuzaki, Open Journal of Composite Materials 2015, 6, 18.
[27] C. Yang, X. Tian, T. Liu, Y. Cao, D. Li, Rapid Prototyping Journal 2017, 23.
[28] X. Tian, T. Liu, C. Yang, Q. Wang, D. Li, Composites Part A: Applied Science and Manufacturing 2016, 88, 198.
[29] B. G. Compton, J. A. Lewis, Advanced Materials 2014, 26, 5930.
[30] K. Kim, W. Zhu, X. Qu, C. Aaronson, W. R. McCall, S. Chen, D. J. Sirbuly, ACS Nano 2014, 8, 9799.
[31] Y. Y. C. Choong, S. Maleksaeedi, H. Eng, J. Wei, P.-C. Su, Materials & Design 2017, 126, 219.
[32] T. Nakamoto, O. Kanehisa, Y. Sugawa, Journal of Advanced Mechanical Design, Systems, and Manufacturing 2013, 7, 888.

[33] L. R. Holmes, J. C. Riddick, JOM 2014, 66, 270.
[34] T. Nakamoto, S. Kojima, Journal of Advanced Mechanical Design, Systems, and Manufacturing 2012, 6, 849.
[35] T. Nakamoto, K. Matsuzaki, Journal ref: International Journal of Automation Technology 2008, 2, 457.
[36] T. Ray, R. Collino, L. Friedrich, J. Cornell, M. Begley, "Field-assisted 3d-printing of aligned composites", presented at *24th International Congress of Theoretical and Applied Mechanics*, Montreal, Canada, 2016.
[37] D. E. Yunus, W. Shi, S. Sohrabi, Y. Liu, Nanotechnology 2016, 27, 495302.
[38] A. Gupta, A. A. Ogale, Polymer composites 2002, 23, 1162.
[39] D. Karalekas, K. Antoniou, Journal of materials processing technology 2004, 153, 526.
[40] D. E. Karalekas, Materials & design 2003, 24, 665.
[41] S. Yuan, J. Bai, K. C. Chua, J. Wei, K. Zhou, Polymers 2016, 8.
[42] R. D. Goodridge, M. L. Shofner, R. J. M. Hague, M. McClelland, M. R. Schlea, R. B. Johnson, C. J. Tuck, Polymer Testing 2011, 30, 94.
[43] K. V. Wong, A. Hernandez, ISRN Mechanical Engineering 2012, 2012, Article ID 208760.
[44] D. Klosterman, R. Chartoff, G. Graves, N. Osborne, B. Priore, Composites Part A: Applied Science and Manufacturing 1998, 29, 1165.
[45] Impossible-Objects.
[46] B. N. Turner, S. A. Gold, Rapid Prototyping Journal 2015, 21, 250.
[47] A. Plymill, R. Minneci, D. A. Greeley, J. Gritton, University of Tennessee Honors Thesis Projects, Graphene and carbon nanotube PLA composite feedstock development for fused deposition, University of Tennessee Honors Thesis Projects, 2016.
[48] S. Dul, L. Fambri, A. Pegoretti, Composites Part A: Applied Science and Manufacturing 2016, 85, 181.
[49] X. Wei, D. Li, W. Jiang, Z. Gu, X. Wang, Z. Zhang, Z. Sun, Scientific Reports 2015, 5, 11181, 1.
[50] R. W. Gray IV, D. G. Baird, J. Helge Bøhn, Rapid Prototyping Journal 1998, 4, 14.
[51] R. W. Gray, D. G. Baird, J. H. Bøhn, Polymer composites 1998, 19, 383.
[52] W. Zhong, F. Li, Z. Zhang, L. Song, Z. Li, Materials Science and Engineering: A 2001, 301, 125.
[53] M. Milosevic, D. Stoof, K. Pickering, Journal of Composites Science 2017, 1, 7.
[54] F. Ning, W. Cong, J. Qiu, J. Wei, S. Wang, Composites Part B: Engineering 2015, 80, 369.
[55] M. Nikzad, S. H. Masood, I. Sbarski, Materials & Design 2011, 32, 3448.
[56] S. H. Masood, W. Q. Song, Materials & Design 2004, 25, 587.
[57] K. C. Chuang, J. E. Grady, S. M. Arnold, R. D. Draper, E. Shin, C. Patterson, T. Santelle, C. Lao, M. Rhein, J. Mehl, NASA Technical reports server 2015, 20150011644
[58] A. A. Stepashkin, D. I. Chukov, F. S. Senatov, A. I. Salimon, A. M. Korsunsky, S. D. Kaloshkin, Composites Science and Technology, 164, 319.
[59] R. Luchoo, L. Harper, M. Bond, N. Warrior, A. Dodworth, Plastics, Rubber and Composites 2010, 39, 216.
[60] G. Liao, Z. Li, Y. Cheng, D. Xu, D. Zhu, S. Jiang, J. Guo, X. Chen, G. Xu, Y. Zhu, Materials & Design 2018, 139, 283.
[61] S. Dul, L. Fambri, A. Pegoretti, Nanomaterials 2018, 8, 49.
[62] S. Berretta, R. Davies, Y. T. Shyng, Y. Wang, O. Ghita, Polymer Testing 2017, 63, 251.
[63] N. Li, Y. Li, S. Liu, Journal of Materials Processing Technology 2016, 238, 218.
[64] M. Namiki, M. Ueda, A. Todoroki, Y. Hirano, R. Matsuzaki, "3D printing of continuous fiber reinforced plastic", presented at *Proceedings of the Society of the Advancement of Material and Process Engineering*, Seattle, WA, USA, 2014.
[65] K. Mori, T. Maeno, Y. Nakagawa, Procedia Engineering 2014, 81, 1595.
[66] Y. Nakagawa, K. Mori, T. Maeno, The International Journal of Advanced Manufacturing Technology 2017, 91, 2811.
[67] W. Zhong, F. Li, Z. Zhang, L. Song, Z. Li, Materials and Manufacturing Processes 2001, 16, 17.

[68] G. W. Melenka, B. K. O. Cheung, J. S. Schofield, M. R. Dawson, J. P. Carey, Composite Structures 2016, 153, 866.
[69] J. M. Gardner, G. Sauti, J. W. Kim, R. J. Cano, R. A. Wincheski, C. J. Stelter, B. W. Grimsley, D. C. Working, E. J. Siochi, in *SAMPE 2016*, Long Beach, CA, United States 2016; J. M. Gardner, G. Sauti, J.-W. Kim, R. J. Cano, R. A. Wincheski, C. J. Stelter, B. W. Grimsley, D. C. Working, E. J. Siochi, Additive Manufacturing 2016, 12, Part A, 38.
[70] J. Justo, L. Távara, L. García-Guzmán, F. París, Composite Structures 2018, 185, 537.
[71] G. D. Goh, V. Dikshit, A. P. Nagalingam, G. L. Goh, S. Agarwala, S. L. Sing, J. Wei, W. Y. Yeong, Materials & Design 2018, 137, 79.
[72] W. Hao, Y. Liu, H. Zhou, H. Chen, D. Fang, Polymer Testing 2018, 65, 29.
[73] G. Postiglione, G. Natale, G. Griffini, M. Levi, S. Turri, Composites Part A: Applied Science and Manufacturing 2015, 76, 110.
[74] M. Invernizzi, G. Natale, M. Levi, S. Turri, G. Griffini, Materials 2016, 9, 583.
[75] G. Griffini, M. Invernizzi, M. Levi, G. Natale, G. Postiglione, S. Turri, Polymer 2016, 91, 174.
[76] J. H. Kim, S. Lee, M. Wajahat, H. Jeong, W. S. Chang, H. J. Jeong, J. R. Yang, J. T. Kim, S. K. Seol, ACS nano 2016, 10, 8879.
[77] C. M. Cheah, J. Y. H. Fuh, A. Y. C. Nee, L. Lu, Rapid Prototyping Journal 1999, 5, 112.
[78] P. Tesavibul, R. Felzmann, S. Gruber, R. Liska, I. Thompson, A. R. Boccaccini, J. Stampfl, Materials Letters 2012, 74, 81.
[79] M. Gurr, D. Hofmann, M. Ehm, Y. Thomann, R. Kübler, R. Mülhaupt, Advanced Functional Materials 2008, 18, 2390.
[80] A. Chiappone, I. Roppolo, E. Naretto, E. Fantino, F. Calignano, M. Sangermano, F. Pirri, Composites Part B: Engineering 2017, 124, 9.
[81] S. H. Chiu, S. T. Wicaksono, K. T. Chen, C. Y. Chen, S. H. Pong, Rapid Prototyping Journal 2015, 21, 262.
[82] C. Provin, S. Monneret, Electronics Packaging Manufacturing, IEEE Transactions on 2002, 25, 59.
[83] Z. L. Lu, F. Lu, J. W. Cao, D. C. Li, Materials and Manufacturing Processes 2014, 29, 201.
[84] V. R. Gervasi, R. S. Crockett, "Composites with gradient properties from solid freeform fabrication", presented at *Solid Freeform Fabrication Symposium*, 1998.
[85] A. A. Ogale, T. Renault, R. L. Dooley, A. Bagchi, C. C. Jara-Almonte, SAMPE quarterly 1991, 23, 28.
[86] T. Renault, A. Ogale, ANTEC 92--Shaping the Future. 1992, 1, 745.
[87] R. Nagalingam, S. Sundaram, B. Stanly, J. Retnam, Bulletin of Materials Science 2010, 33, 525.
[88] A. Sakly, S. Kenzari, D. Bonina, S. Corbel, V. Fournée, Materials & Design 2014, 56, 280.
[89] V. K. Popov, A. V. Evseev, A. L. Ivanov, V. V. Roginski, A. I. Volozhin, S. M. Howdle, Journal of Materials Science: Materials in Medicine 2004, 15, 123.
[90] G. Zak, A. Y. F. Chan, C. B. Park, B. Benhabib, Rapid Prototyping Journal 1996, 2, 16.
[91] G. Zak, M. N. Sela, V. Yevko, C. B. Park, B. Benhabib, Journal of manufacturing science and engineering 1999, 121, 448.
[92] G. Zak, M. Haberer, C. B. Park, B. Benhabib, Rapid Prototyping Journal 2000, 6, 107.
[93] M. Haberer, G. Zak, C. B. Park, B. Benhabib, Journal of manufacturing science and engineering 2003, 125, 564; M. Haberer, G. Zak, C. B. Park, M. Paraschivoiu, B. Benhabib, Proceedings of the Institution of Mechanical Engineers, Part C: Journal of Mechanical Engineering Science 2003, 217, 65.
[94] C. Greer, J. McLaurin, A. A. Ogale, "Processing of carbon fiber reinforced composites by three dimensional photolithography", presented at *Proc. Solid Freeform Fabrication Symp., Texas*, 1996.
[95] J. Fuh, Y. Choo, L. Lu, A. Nee, Y. Wong, W. Wang, T. Miyazawa, S. Ho, Journal of materials processing technology 1997, 63, 887; G. Salmoria, C. Ahrens, V. Beal, A. Pires, V. Soldi, Materials & Design 2009, 30, 758.

[96] D. Klosterman, R. P. Chartoff, N. R. Osborne, G. Graves, A. Lightman, G. Han, A. Bezeredi, S. Rodrigues, S. Pak, G. Kalmanovich, "Curved layer LOM of ceramics and composites", presented at *Solid Freeform Fabrication Symposium proceedings. University of Texas, Austin*, 1998.
[97] M. Chapiro, Reinforced Plastics 2016, 60, 372.
[98] W. Zhu, C. Yan, Y. Shi, S. Wen, J. Liu, Q. Wei, Y. Shi, Scientific Reports 2016, 6, 33780.
[99] J. Bai, R. D. Goodridge, R. J. M. Hague, M. Song, H. Murakami, Journal of Materials Research 2014, 29, 1817.
[100] S. R. Athreya, K. Kalaitzidou, S. Das, Composites Science and Technology 2011, 71, 506.
[101] M. S. Wahab, K. W. Dalgarno, B. Cochrane, Journal of Mechanics Engineering and Automation 2011, 1, 100.
[102] H. Chung, S. Das, Materials Science and Engineering: A 2006, 437, 226.
[103] T. H. C. Childs, N. P. Juster, CIRP Annals - Manufacturing Technology 1994, 43, 163; P. Forderhase, K. McAlea, R. Booth, "The development of a SLS® composite material", presented at *Proceedings of the solid freeform fabrication symposium*, Austin Texas, 1995.
[104] K. K. B. Hon, T. J. Gill, CIRP Annals - Manufacturing Technology 2003, 52, 173.
[105] T. J. Gill, K. K. B. Hon, Proceedings of the Institution of Mechanical Engineers, Part B: Journal of Engineering Manufacture 2004, 218, 1249.
[106] Y. Chunze, S. Yusheng, Y. Jinsong, L. Jinhui, Journal of Reinforced Plastics and Composites 2008, 28, 2889.
[107] Y. Laixia, W. Bo, Z. Wenming, IOP Conference Series: Materials Science and Engineering 2017, 274, 012118.
[108] Y. Chun-Ze, S. Yu-Sheng, Y. Jing-Song, X. Lin, Journal of Composite Materials 2009, 43, 1835.
[109] A. Salazar, A. Rico, J. Rodríguez, J. Segurado Escudero, R. Seltzer, F. Martin de la Escalera Cutillas, Composites Part B: Engineering 2014, 59, 285.
[110] S. Arai, S. Tsunoda, R. Kawamura, K. Kuboyama, T. Ougizawa, Materials & Design 2017, 113, 214.
[111] S. M. Lebedev, O. S. Gefle, E. T. Amitov, D. V. Zhuravlev, D. Y. Berchuk, E. A. Mikutskiy, The International Journal of Advanced Manufacturing Technology 2018.
[112] L. Xionghao, N. Zhongjin, B. Shuyang, L. Baiyang, IOP Conference Series: Materials Science and Engineering 2018, 322, 022012.
[113] W. Zhang, C. Cotton, J. Sun, D. Heider, B. Gu, B. Sun, T.-W. Chou, Composites Part B: Engineering 2018, 137, 51.
[114] M. Araya-Calvo, I. López-Gómez, N. Chamberlain-Simon, J. L. León-Salazar, T. Guillén-Girón, J. S. Corrales-Cordero, O. Sánchez-Brenes, Additive Manufacturing 2018, 22, 157.
[115] X. Tian, T. Liu, Q. Wang, A. Dilmurat, D. Li, G. Ziegmann, Journal of Cleaner Production 2017, 142, 1609.
[116] D. Jiang, D. Smith, "Mechanical Behavior of Carbon Fiber Composites Produced with Fused Filament Fabrication", presented at *Solid Freeform Fabrication 2016: Proceedings of the 26th Annual International Solid Freeform Fabrication Symposium – An Additive Manufacturing Conference*, Texas, USA, 2016.
[117] M. A. Caminero, J. M. Chacón, I. García-Moreno, G. P. Rodríguez, Composites Part B: Engineering 2018, 148, 93.
[118] T. H. J. Vaneker, Procedia CIRP 2017, 66, 317.
[119] R. Charan, T. Renault, A. A. Ogale, A. Bagchi, "Automated fiber-reinforced composite prototypes", presented at *Fifth International Conference on Rapid Prototyping*, 1994.
[120] F. R. Bruce, H. Gene, F. Kent, Rapid Prototyping Journal 2009, 15, 339.
[121] W. Jing, C. Hui, W. Qiong, L. Hongbo, L. Zhanjun, Materials & Design 2017, 116, 253.
[122] D.-A. Türk, F. Brenni, M. Zogg, M. Meboldt, Materials & Design 2017, 118, 256.
[123] R. G. Kleijnen, J. P. W. Sesseg, M. Schmid, K. Wegener, AIP Conference Proceedings 2017, 1914, 190002.
[124] D. V. Isakov, Q. Lei, F. Castles, C. J. Stevens, C. R. M. Grovenor, P. S. Grant, Materials & Design 2016, 93, 423.

[125] F. Castles, D. Isakov, A. Lui, Q. Lei, C. E. J. Dancer, Y. Wang, J. M. Janurudin, S. C. Speller, C. R. M. Grovenor, P. S. Grant, Scientific Reports 2016, 6, 22714; D. Roper, B. Good, S. Yarlagadda, M. Mirotznik, "Fabrication of flat Luneburg lens using functional additive manufacturing", presented at *2014 USNC-URSI Radio Science Meeting (Joint with AP-S Symposium)*, 6-11 July 2014, 2014.
[126] J. Zhang, J. Li, S. Chen, N. Kawazoe, G. Chen, Journal of Materials Chemistry B 2016, 4, 5664; J. Zhang, S. Zhao, M. Zhu, Y. Zhu, Y. Zhang, Z. Liu, C. Zhang, Journal of Materials Chemistry B 2014, 2, 7583.
[127] M. Sugavaneswaran, G. Arumaikkannu, Materials & Design 2015, 66, 29; M. Sugavaneswaran, G. Arumaikkannu, Materials & Design 2014, 54, 779; Y. L. Yap, V. Dikshit, S. P. Lionar, H. Yang, J. C. Lim, X. Qi, W. Y. Yeong, J. Wei, "Investigation of fiber reinforced composite using multi-material 3d printing", presented at *2016 Annual International Solid Freeform Fabrication Symposium*, Austin, TX, USA, 2016.
[128] A. Fischer, S. Rommel, A. Verl, in *Soft Robotics: Transferring Theory to Application*, (Eds: A. Verl, A. Albu-Schäffer, O. Brock, A. Raatz), Springer Berlin Heidelberg, Berlin, Heidelberg 2015, 198; N. W. Bartlett, M. T. Tolley, J. T. B. Overvelde, J. C. Weaver, B. Mosadegh, K. Bertoldi, G. M. Whitesides, R. J. Wood, Science 2015, 349, 161; Y. Mao, Z. Ding, C. Yuan, S. Ai, M. Isakov, J. Wu, T. Wang, M. L. Dunn, H. J. Qi, Scientific Reports 2016, 6, 24761; A. Zolfagharian, A. Z. Kouzani, S. Y. Khoo, A. A. A. Moghadam, I. Gibson, A. Kaynak, Sensors and Actuators A: Physical 2016, 250,

258.
[129] L. Djumas, A. Molotnikov, G. P. Simon, Y. Estrin, Scientific Reports 2016, 6, 26706; F. Libonati, G. X. Gu, Z. Qin, L. Vergani, M. J. Buehler, Advanced Engineering Materials 2016, 18, 1354; L. S. Dimas, M. J. Buehler, Soft Matter 2014, 10, 4436.
[130] K. Wang, Y. Zhao, Y.-H. Chang, Z. Qian, C. Zhang, B. Wang, M. A. Vannan, M.-J. Wang, Materials & Design 2016, 90, 704; K. Wang, C. Wu, Z. Qian, C. Zhang, B. Wang, M. A. Vannan, Additive Manufacturing 2016, 12, Part A, 31.
[131] Q. Ge, H. J. Qi, M. L. Dunn, Applied Physics Letters 2013, 103, 131901; Q. Zhao, H. J. Qi, T. Xie, Progress in Polymer Science 2015, 49–50, 79; J. Wu, C. Yuan, Z. Ding, M. Isakov, Y. Mao, T. Wang, M. L. Dunn, H. J. Qi, Scientific Reports 2016, 6, 24224.
[132] W. Tao, M. C. Leu, "Design of lattice structure for additive manufacturing", presented at *2016 International Symposium on Flexible Automation (ISFA)*, Cleveland, Ohio, 2016.
[133] Y. L. Yap, Y. M. Lai, H. F. Zhou, W. Y. Yeong, "Compressive strength of thin-walled cellular core by inkjet-based additive manufacturing", presented at *Proceedings of the 1st International Conference on Progress in Additive Manufacturing (Pro-AM 2014)*, Singapore, 2014.
[134] V. Dikshit, N. A. Prasanth, J. D. Kumar, Y. L. Yap, W. Y. Yeong, "Investigation of quasi static indentation on 3D printed honeycomb based truncated-pyramid square structure", presented at *Proceedings of the 2nd International Conference on Progress in Additive Manufacturing (Pro-AM 2016)*, Singapore, 2016; V. Dikshit, N. A. Prasanth, J. D. Kumar, Y. L. Yap, S. Agarwala, W. Y. Yeong, "Out of plane compressive strength of 3D printed vertical pillared corrugated core structure", presented at *Proceedings of the 2nd International Conference on Progress in Additive Manufacturing (Pro-AM 2016)*, Singapore, 2016.
[135] V. Dikshit, Y. L. Yap, G. D. Goh, H. Yang, J. C. Lim, X. Qi, W. Y. Yeong, J. Wei, "Investigation of out of plane compressive strength of 3D printed sandwich composites", presented at *IOP Conference Series: Materials Science and Engineering*, 2016. .
[136] Y. C. Zhang, X. Wang, International Journal of Solids and Structures 2005, 42, 5399.
[137] Y. X. Gan, International Journal of Molecular Sciences 2009, 10, 5115.
[138] L. Liu, C. Jia, J. He, F. Zhao, D. Fan, L. Xing, M. Wang, F. Wang, Z. Jiang, Y. Huang, Composites Science and Technology 2015, 121, 56.
[139] X. Xu, M. M. Thwe, C. Shearwood, K. Liao, Applied physics letters 2002, 81, 2833.
[140] V. Lordi, N. Yao, Journal of Materials Research 2011, 15, 2770.
[141] P.-C. Ma, N. A. Siddiqui, G. Marom, J.-K. Kim, Composites Part A: Applied Science and Manufacturing 2010, 41, 1345; L. G. Tang, J. L. Kardos, Polymer composites 1997, 18, 100.
[142] C. Yan, L. Hao, L. Xu, Y. Shi, Composites Science and Technology 2011, 71, 1834.
[143] X. Jining, Z. Nanyan, G. Manton, K. V. Vijay, Smart Materials and Structures 2002, 11, 575.

[144] D. Filgueira, S. Holmen, J. K. Melbø, D. Moldes, A. T. Echtermeyer, G. Chinga-Carrasco, ACS Sustainable Chemistry & Engineering 2017, 5, 9338.
[145] J. L. Figueiredo, M. F. R. Pereira, M. M. A. Freitas, J. J. M. Órfão, Carbon 1999, 37, 1379.
[146] A. Dong, Y. Yu, J. Yuan, Q. Wang, X. Fan, Applied Surface Science 2014, 301, 418.
[147] J. Garcia-Ubasart, A. Esteban, C. Vila, M. B. Roncero, J. F. Colom, T. Vidal, Bioresource Technology 2011, 102, 2799.
[148] X. Ni, A. Dong, X. Fan, Q. Wang, Y. Yu, A. Cavaco-Paulo, Fibers and Polymers 2015, 16,

2276.
[149] X. Ni, A. Dong, X. Fan, Q. Wang, Y. Yu, A. Cavaco-Paulo, Polymer Composites 2017, 38, 1327.
[150] J. H. Sandoval, K. F. Soto, L. E. Murr, R. B. Wicker, Journal of Materials Science 2007, 42, 156.
[151] S. Christ, M. Schnabel, E. Vorndran, J. Groll, U. Gbureck, Materials Letters 2015, 139, 165.
[152] G. C. Pidcock, M. in het Panhuis, Advanced Functional Materials 2012, 22, 4790.
[153] J. P. Lewicki, J. N. Rodriguez, C. Zhu, M. A. Worsley, A. S. Wu, Y. Kanarska, J. D. Horn, E. B. Duoss, J. M. Ortega, W. Elmer, R. Hensleigh, R. A. Fellini, M. J. King, Scientific Reports 2017, 7, 43401.
[154] D. Yang, K. Wu, L. Wan, Y. Sheng, Journal of Manufacturing and Materials Processing 2017, 1, 10.
[155] Y. Doruk Erdem, S. Wentao, S. Salman, L. Yaling, Nanotechnology 2016, 27, 495302.
[156] R. M. Erb, R. Libanori, N. Rothfuchs, A. R. Studart, Science 2012, 335, 199; L. Lu, P. Guo, Y. Pan, Journal of Manufacturing Science and Engineering 2017.
[157] M. L.-J. Thomas, W. D. Bruce, S. T. Richard, Smart Materials and Structures 2016, 25, issue: 2; M. S. Scholz, B. W. Drinkwater, R. S. Trask, Ultrasonics 2014, 54, 1015; Y. Doruk Erdem, S. Salman, H. Ran, S. Wentao, L. Yaling, Journal of Micromechanics and Microengineering 2017, 27, 045016.
[158] A. N. Dickson, J. N. Barry, K. A. McDonnell, D. P. Dowling, Additive Manufacturing 2017, 16, 146.
[159] K. Agarwal, S. K. Kuchipudi, B. Girard, M. Houser, Journal of Composite Materials 2018, 0021998318762297.
[160] A. Le Duigou, M. Castro, R. Bevan, N. Martin, Materials & Design 2016, 96, 106.
[161] M. Domm, J. Schlimbach, P. Mitschang, "OPTIMIZING MECHANICAL PROPERTIES OF ADDITIVELY MANUFACTURED FRPC", presented at *21st International Conference on Composite Materials*, Xi'an, China.
[162] N. Aliheidari, R. Tripuraneni, A. Ameli, S. Nadimpalli, Polymer Testing 2017, 60, 94.
[163] M. A. Caminero, J. M. Chacón, I. García-Moreno, J. M. Reverte, Polymer Testing 2018, 68, 415.
[164] B. Van Hooreweder, D. Moens, R. Boonen, J.-P. Kruth, P. Sas, Polymer Testing 2013, 32, 972.
[165] J. Mueller, K. Shea, "The effect of build orientation on the mechanical properties in inkjet 3D-printing", presented at *International Solid Freeform Fabrication Symposium*, 2015.
[166] A. C. Abbott, G. P. Tandon, R. L. Bradford, H. Koerner, J. W. Baur, Additive Manufacturing 2018, 19, 29.
[167] D. Young, J. Kessler, M. Czabaj, "Interlayer fracture toughness of additively manufactured unreinforced and carbon-fiber-reinforced acrylonitrile butadiene styrene", presented at *31st Annual Technical Conference of the American Society for Composites, ASC 2016*, 2016.
[168] D. J. Radcliffe, H. M. Rosenberg, Cryogenics 1982, 22, 245.
[169] A. K. Ravi, A. Deshpande, K. H. Hsu, Journal of Manufacturing Processes 2016, 24, 179.
[170] M. Zhang, X. Song, W. Grove, E. Hull, Z. J. Pei, F. Ning, W. Cong, "Carbon nanotube reinforced fused deposition modeling using microwave irradiation", presented at *ASME 2016 11th International Manufacturing Science and Engineering Conference*, Blacksburg, Virginia, USA, 2016.
[171] Q. Sun, G. M. Rizvi, C. T. Bellehumeur, P. Gu, Rapid Prototyping Journal 2008, 14, 72.
[172] P. Parandoush, L. Tucker, C. Zhou, D. Lin, Materials & Design 2017, 131, 186.

[173] Z. Quan, A. Wu, M. Keefe, X. Qin, J. Yu, J. Suhr, J.-H. Byun, B.-S. Kim, T.-W. Chou, Materials Today 2015, 18, 503.
[174] T. Stichel, T. Frick, T. Laumer, F. Tenner, T. Hausotte, M. Merklein, M. Schmidt, Optics & Laser Technology 2017, 89, 31.
[175] K. C. Chuang, J. E. Grady, R. D. Draper, E.-S. E. Shin, C. Patterson, T. D. Santelle, "Additive manufacturing and characterization of Ultem polymers and composites", presented at *CAMX Conference Proceedings*, Dallas, TX, USA, October 26-29, 2015.
[176] S. A. Ntim, O. Sae-Khow, F. A. Witzmann, S. Mitra, Journal of Colloid and Interface Science 2011, 355, 383.
[177] A. Lucas, C. Zakri, M. Maugey, M. Pasquali, P. Van Der Schoot, P. Poulin, The Journal of Physical Chemistry C 2009, 113, 20599; J. Yu, N. Grossiord, C. E. Koning, J. Loos, Carbon 2007, 45, 618.
[178] B. Y. Ahn, E. B. Duoss, M. J. Motala, X. Guo, S.-I. Park, Y. Xiong, J. Yoon, R. G. Nuzzo, J. A. Rogers, J. A. Lewis, Science 2009, 323, 1590.
[179] K. Sun, T.-S. Wei, B. Y. Ahn, J. Y. Seo, S. J. Dillon, J. A. Lewis, Advanced Materials 2013, 25, 4539.
[180] Z. Weng, Y. Zhou, W. Lin, T. Senthil, L. Wu, Composites Part A: Applied Science and Manufacturing 2016, 88, 234.
[181] S. Wang, L. Capoen, D. R. D'hooge, L. Cardon, Plastics, Rubber and Composites 2018, 47, 9.
[182] L. Verbelen, S. Dadbakhsh, M. Van den Eynde, J.-P. Kruth, B. Goderis, P. Van Puyvelde, European Polymer Journal 2016, 75, 163.
[183] J. Bai, R. D. Goodridge, R. J. M. Hague, M. Song, M. Okamoto, Polymer Testing 2014, 36, 95.
[184] S. Song, M. Park, J. Lee, J. Yun, Nanomaterials 2018, 8, 93.
[185] X. Song, 2016.
[186] K. Lozano, J. Bonilla-Rios, E. V. Barrera, Journal of Applied Polymer Science 2001, 80, 1162.
[187] J. Nelson, University of Texas at Austin, 1993.
[188] H. Chung, University of Michigan, 2005.
[189] H. Bikas, P. Stavropoulos, G. Chryssolouris, The International Journal of Advanced Manufacturing Technology 2016, 83, 389.
[190] B. N. Turner, R. Strong, S. A. Gold, Rapid Prototyping Journal 2014, 20, 192.
[191] M. Yosofi, O. Kerbrat, P. Mognol, Virtual and Physical Prototyping 2018, 13, 83.
[192] K. Zeng, D. Pal, B. Stucker, "A review of thermal analysis methods in Laser Sintering and Selective Laser Melting", presented at *Proceedings of Solid Freeform Fabrication Symposium Austin, TX*, 2012.
[193] L. Flach, M. A. Jacobs, D. A. Klosterman, R. Chartoff, "'Simulation of Laminated Object Manufacturing LOM with Variation of Process Parameters", presented at *Proceedings of Solid Freeform Fabrication Symposium*, 1998.
[194] D. Klosterman, L. Flach, E. Bryant, R. Chartoff, "Development and Verification of a Thermal Model for a Novel Automated Composite Fabrications Process: Laminated Object Manufacturing (LOM)", presented at *The 12nd International Conference on Composites (ICCM-12)*, Paris, France, 2000.
[195] L. Flach, E. Bryant, D. Klosterman, R. Chartoff, "A Mathematical Model for Optimal Control of Cure Distribution in Parts Made by Laminated Object Fabrication (LOF)", presented at *Bridging the Centuries with SAMPE's Materials and Processes Technology: Long Beach Convention Center, Long Beach California, May 21-25, 2000*, 2000.
[196] D. Brackett, I. Ashcroft, R. Hague, "Topology optimization for additive manufacturing", presented at *Proceedings of the solid freeform fabrication symposium, Austin, TX*, 2011; M. Tomlin, J. Meyer, "Topology optimization of an additive layer manufactured (ALM) aerospace part", presented at *Proceeding of the 7th Altair CAE technology conference*, 2011.
[197] A. Garg, K. Tai, M. Savalani, Rapid Prototyping Journal 2014, 20, 164.
[198] R. Joven, R. Das, A. Ahmed, P. Roozbehjavan, B. Minaie, SAMPE, Charleston, SC 2012.
[199] 2017.

Figure Captions

Figure 1 Classification of different AM processes for FRPC

Figure 2 Material extrusion process: (a) fused filament fabrication, (b) liquid deposition modelling.

Figure 3 Tensile strength vs fiber volume ratio of parts manufactured via various conventional and AM techniques

Figure 4 Vat-photopolymerization process and the schematic representation of the cross-sectional view of the UV curing of FRPC in SLA.

Figure 5 Sheet lamination process: (a) laminated object manufacturing (LOM) and (b) composite-based additive manufacturing.

Figure 6 Schematic representation of powder bed fusion and the composite powder used.

Tables

Table 1 – Summary of various AM techniques for FRPC

Author Biography

GOH Guo Dong received his Bachelor's degree in Aerospace Engineering from Nanyang Technological University (NTU), Singapore in 2015. He is currently pursuing his Ph.D. degree at the School of Mechanical and Aerospace Engineering, NTU. His current research works focus on additively manufactured continuous fiber reinforced thermoplastics composite via extrusion based technique

YAP Yee Ling received her Bachelor's degree in Aerospace Engineering from Nanyang Technological University (NTU), Singapore in 2015. She is currently pursuing her Ph.D. degree at the School of Mechanical and Aerospace Engineering, NTU. Her current research works focus on fiber reinforced Multi-material for soft robotics.

Shweta AGARWALA obtained her Ph.D. in electronics engineering in 2012 from National University of Singapore (NUS) on nanostructured materials for dye-sensitized solar cells. Currently, she is a research fellow at SC3DP, NTU. Her research is aimed at printed electronics, 3D printing, bioprinting and materials for electronics, biomedical and aerospace applications.

YEONG Wai Yee is an Assistant Professor in school of Mechanical and Aerospace engineering, Nanyang Technological University. Her main research interest is in 3D printing and bioprinting of multi-functional structures, printed electronics and bio-electronic platforms. She has published 2 textbooks in 3D printing and her H-index is 18. She is the associate editor for 2 international journals which are indexed in ESCI web-of-science database.